Phosphorus spatial distribution and mass balance in the Itaipu lagoon (Rio de Janeiro, Brazil)

Marcelo Lobo[1], Daniel Loureiro[1], Aguinaldo Nepomuceno[1], Leandro Alves[1], Fernando Lamego[1,2]*

[1] Universidade Federal Fluminense - Programa de Biologia Marinha e Ambientes Costeiros (Campus do Valonguinho, CP 100.644 - Niterói - 24001-970 - RJ - Brazil)

[2] Instituto de Engenharia Nuclear, Comissão Nacional de Energia Nuclear (Rua Hélio de Almeida, 75 - Cidade Universitária - Ilha do Fundão - Caixa Postal 68550 - Rio de Janeiro - 21941-906 - RJ - Brazil)

* Corresponding author: flamego@ien.gov.br

ABSTRACT

The degradation of tropical coastal lagoon systems in urban areas of the least developed countries has been associated with an increase in impermeable areas and poor domestic sewage treatment, increasing land-based runoff of nutrients and suspended solids from catchments. This study aimed to assess the biogeochemical changes caused by human interventions through the analysis of the spatial distribution of sedimentary phosphorus (P) and its mass balance in the Itaipu lagoon, located on the east coast of the state of Rio de Janeiro. Human intervention in the Itaipu lagoon system has caused severe imbalances in biogeochemical cycles over the past decades. Watercourses have been channeled to normalize the hydrological regime and increase hydraulic energy, improving sediment transport capacity. In this context, the increase in runoff from the coastal urban basin into the Itaipu lagoon has buried an increasing amount of phosphorus in the sediment. Recently, a regional increase in storm events caused a series of landslides and floods, which have been reported as possible consequences of global climate change. In recent decades, the synergy between landslides and river channeling has increased TP loads, accelerating phosphorus settling and changing P spatial distribution in surface sediments. This has accelerated siltation of the lagoon with an accumulation of nutrients and organic matter, leading in some cases to sediment anoxia. The lagoon has undergone strong eutrophication, changing its trophic state from meso- to hypertrophic in less than 30 years, even though P loads are not as high as in other coastal lagoons. Our findings confirm that human intervention impacts nutrient loads, which in turn disrupt the balance of biogeochemical cycles, compromising coastal water resources. This leads to the collapse of ecosystem services, another step towards degrading planetary boundaries.

Descriptors: Phosphorus loads, Domestic sewage, Eutrophication, Sedimentation, Coastal lagoon.

INTRODUCTION

Coastal lagoons are often found in coastal zones worldwide and are classified as bar-built estuaries. These are shallow water bodies that, in general, may or may not have well-defined tidal channels. Such ecosystems are at the land-sea interface and play an important role in the biogeochemical cycle of various elements, as they can accumulate organic matter and nutrients from the continental environment (Pagliosa et al., 2006) with high rates of primary production and respiration as well as high autotrophic and heterotrophic biomass (A. V. . Borges, 2005). Furthermore, part of this autotrophic biomass is exported as phytoplankton-derived organic matter from the lagoon to the continental shelf, supplying nutrients to ocean food chains (Erbas et al., 2021). Many coastal lagoons in the tropics undergo anthropogenic

pressure, particularly from eutrophication induced by untreated or partially treated sewage discharge and accelerated basin erosion. The long-term nutrient accumulation considerably changes coastal lagoon ecosystem structures and trophic states, favoring suboxic and anoxic conditions and leading to aquatic environment degradation.

Eutrophication is highly regulated by phosphorus (P), a limiting nutrient for primary production. This element is rarely found in the free state and is instead retained in phosphate rocks, its main natural reservoir (Ruttenberg, 2003), as well as in organic molecule compositions (Sawyer et al 2003). Rock weathering causes P to return to its biogeochemical cycle in orthophosphate form, whereupon it can be rapidly assimilated by the phytoplankton community (Tiessen, 2008). Adsorption on amorphous Fe oxides/oxyhydroxides (Fe-oxys) has also been shown to be a significant mechanism for removing P, in inorganic form, from the water column (Pratt et al., 2007).

In urban areas, domestic sewage tends to be the main source of P for tropical coastal aquatic environments. Millennium Ecosystem Assessment estimates have suggested that 95% of global net growth will occur in urban areas of the Least Developed Countries (LDCs), where 90–95% of all types of liquid waste and 70% of industrial effluents are untreated (Lee & Diop, 2009). This increase in P levels will generate unprecedented pressure not only on rivers but also on adjacent estuarine and coastal areas (Conley et al., 2009; Paerl et al., 2014), proliferating 'dead zones' worldwide (Diaz & Rosenberg, 2008; Yang & Gruber, 2016). Soon, this high and continuous discharge of nutrients from human activity, together with climate change, is expected to further intensify eutrophication, unbalancing aquatic ecosystems (Nixon, 1995). It is estimated that P concentrations have currently increased 18 to 180 times compared to pristine concentrations due to anthropic action (Statham, 2012). Many authors have used spatially explicit mass-balance of P from different sources in watersheds as an indicator of eutrophication and basin management (Chapra & Dolan, 2012; Kenney et al., 2014; Kim et al., 2013; Meals et al., 2008; Zhang et al., 2013).

Thus, the current processes that control P distribution and accumulation in these coastal lagoons must be better understood. Although

several studies have assessed the trophic state and eutrophication in these ecosystems over past decades (Knoppers et al., 1991; Souza et al., 2003; Marques Jr et al 2006; Cotovicz Junior et al., 2013; Dias et al., 2017), few have focused on the recent P accumulation in tropical coastal lagoon sediment (Cotovicz Junior et al., 2014). In particular, the Itaipu lagoon, located in the city of Niterói and near the Guanabara bay, has experienced a great deal of eutrophication, and its basin has undergone engineering interventions to control floods and landslides, which accelerated degradation of the water body (Salvador & Da Silva, 2002). These works sought not only to dredge and channel the waterways, but also to partially treatment the domestic sewage released into the main river (João Mendes), which directly contributes freshwater into the lagoon. The founding hypotheses of this study are: i) the synergy between landslides, river channeling, vegetation removal, and demographic growth over the past few decades has produced an increase in TP inflow, accelerating P settling, which altered the P spatial distribution in surface sediments due to biogeochemical changes in the sedimentary environment; and ii) the increase in runoff associated with human intervention combined with poor sanitation of the coastal urban basin has buried increasing amounts of P in the sediment, reflected in its mass balance in the Itaipu lagoon. The pH and Eh-mediated processes affecting P composition, from river discharge to the sea connection, were investigated using in-situ and laboratory high spatial-resolution measurements. Therefore, this study addresses the P spatial distribution and its sedimentary environments as well as the mass balance of Total Phosphorus (TP) in the Itaipu lagoon. Findings on the impact of human intervention on P dynamics and its role as a proxy for eutrophication assessment were presented.

METHODS

STUDY AREA

The hydrography of the municipality of Niterói can be divided into three drainage areas: Shore Region, Guanabara Bay, and North Region. The Shore Region has a total area of 46.5 km² and

includes the hydrographic systems that flow into ocean beaches, forming the Piratininga-Itaipu Lagoon System (PILAS), which comprises the hydrographic basins of the Piratininga and Itaipu lagoons, the latter being the object of this study. The area of the Itaipu lagoon drainage basin is approximately 24 km² and has a long-term average flow of 0.85 m³ s⁻¹ (Niterói, 2019). The tributaries that flow into the Itaipu lagoon are the Vala river, the Tiririca creek, the Itacoatiara wall, and João Mendes river. The latter is the main tributary of the Itaipu lagoon, accounting for approximately 60% of the water and continental material reaching it. It is approximately 7 km long, and its springs are within the Darcy Ribeiro municipal ecological reserve and Serra da Tiririca state park (Figure 1). Currently, the João Mendes river has undergone anthropic intervention along almost its entire length, revealing itself as an urban river with striking indicators of domestic pollution. In 1970, the sub-basin of the João Mendes river had an impervious area of 33%. After more than three decades of intense urbanization, ¾ of the sub-basin was already occupied by impervious surfaces (residences, paving, sewage pipe and

water supply network, etc.) (Braga, 2003). A sewage treatment plant with maximum capacity of 294 L s⁻¹ was installed in the vicinity of the Itaipu lagoon in 2004.

The Itaipu lagoon has an area of 1.2 km², a perimeter of 5.3 km, an average depth of 1m, and a water volume of 2.0 x 10⁶ m³ (Kuchler et al., 2005). The residence time to renew half of the lagoon water (T$_{50}$) was estimated at one day (Knoppers et al., 1991), but this rate has decreased due to siltation observed in recent decades. A recent assessment, using the LOICZ model (Dupra, et al. 2000), has shown that residence time can currently reach three days (Angelini et al., 2021). In the lagoon, two water channels were built to reduce flooding, the Camboatá channel connected to the Piratininga lagoon in the 1940s and the Itaipu channel connected to the sea, which has been permanently open since 1979 (Cerda et al., 2013). Thus, the waters flow from the Piratininga lagoon to the Itaipu lagoon, through which the Itaipu channel reaches the sea. After carrying out these interventions, the water bodies of both lagoons were significantly reduced, allowing for the occupation of their shores.
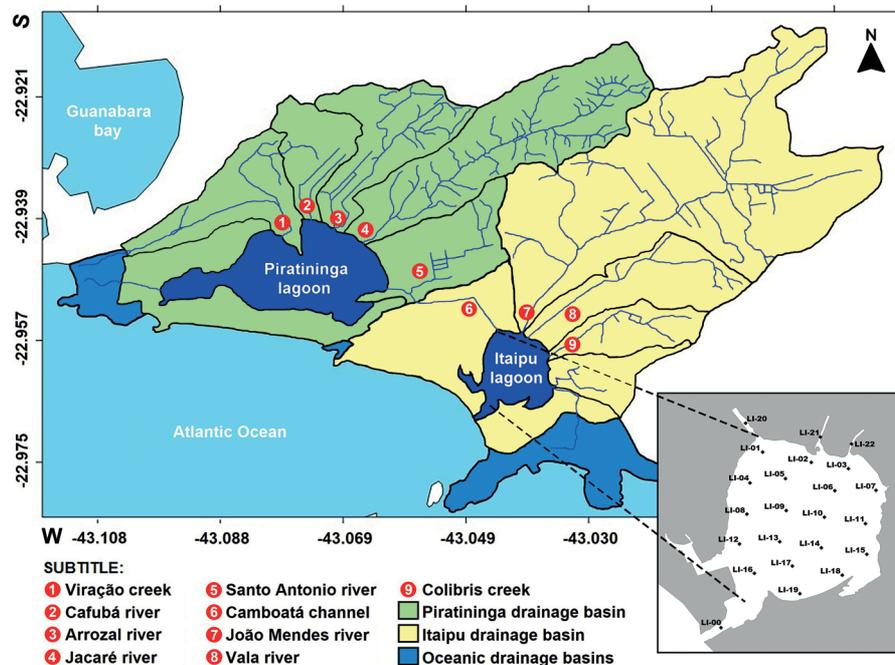

Figure 1. Map of the Piratininga-Itaipu Lagoon System (PILAS), hydrographic basins and respective tributaries. Details about the Itaipu Lagoon and the location of sampling stations can be seen in the lower right corner.

Three seawater masses act in the Itaipu inlet: Tropical Water (TW) from the Brazilian Current, Coastal Water (CW), and South Atlantic Central Water (SACW). There is a predominance of CW on the east coast of the state of Rio de Janeiro. This hydrodynamic influences water circulation within the lagoon, which is dominated by waves with a semi-diurnal micro-tide regime and maximum amplitude of 1.4m in spring tides (DHN, 1987). Transport by coastal currents is stable, with velocities rarely exceeding 10 m s^{-1} and the tidal current predominating within the Itaipu channel (Gallissaires, et al, 1990). The flow of these waters are directly controlled by the tidal cycle in the portions of the lagoon close to the channel. However, the TW circulation is related to upwelling short-term events, with the entry of SACW underneath it into the coastal areas. (Castelao et al., 2004) found that upwelling/downwelling in the coastal area is mainly caused by wind, whereas TW eddies generate vertical velocities over the continental shelf in the South Brazil Bight and are associated with cyclonic meanders of the Brazil current. This vortex-induced upward movement takes the SACW to shallower depths, where it is influenced by wind. When both effects combine, the SACW penetrates all the way to the coast. In addition, these short-term events (3-5 days), which occur during the spring and summer months, were recorded in a recent study in the Saquarema lagoon, also located on the east coast of the state (Erbas et al 2021).

The local climate is classified as sub-humid, with little or no water deficit, and mega thermal with heat well distributed throughout the year (Awi type according to Köepen's classification). There is a dry period from June to September, when average rainfall does not exceed 50 mm, and a rainy period from November to April, with maximum average rainfall in January (> 150 mm). Average seasonal temperatures are between 23 and 31°C during summer, 18 and 26°C during winter, 19 and 27°C during autumn, and 20 and 29°C during spring (Barbieri, 1981).

Sampling design

Surface sediments were sampled from homogeneously distributed sites, covering all morphological features of the lagoon including the mouth of its main tributaries and the edges of local mangroves. Dredged areas were excluded from the sampling net to avoid dealing with scrambled sediments. An aluminum vessel with an outboard motor was used to access sampling points, which were GPS georeferenced (Figure 1). Twenty-two stations were sampled in August 2020, 19 of which were within the Itaipu lagoon and three of which were located in the main tributaries, approximately 50m above the mouths. These samples were collected with Van Veen or Ekman grab samplers, depending on the type of sediment found at each station, with simultaneous measurement of water column depth using a graduated rope. Redox potential (Eh) and pH were immediately measured in situ at each collection point with electrodes inserted into the sediment, using a portable pHmeter (model PHP-500). For pH, a resin electrode calibrated with NIST standard buffer solutions (4.00; 7.00; 10.00) was used. For Eh, a platinum electrode calibrated with a 240 mV solution was used. Both calibrations were performed immediately prior to the sampling. All samples were placed in plastic bags and transported to the laboratory in an icebox.

Analytical procedures

Total phosphorus (TP) and inorganic phosphorus (IP) were extracted and measured (Aspila et al., 1976) using a HITACHI model U-1100 spectrophotometer. TP was extracted from dry pulverized sediment previously ashed in a muffle furnace (450 °C; 4 h), using 10 mL of 1 mol L^{-1} HCl for 16h. Similarly, IP was determined identically to the TP, though without ashing sediment samples. Organic Matter (OM) content was determined by weight loss on ignition (LOI) after combustion at 550 °C for 2h. Organic phosphorus (OP) was derived by subtracting TP from IP. Analyses were carried out in duplicate, and the reproducibility was within 5% for all analyses, as indicated by relative percentage differences calculated for each sample. Measurements of NIST 1646a did not differ from certified values (TP = 0.027 ± 0.001 %) by more than ±5 % of P.

Grain-size analyses were performed in a sieve (63 μm) after organic matter removal by peroxide

attack H_2O_2. By comparing the fraction retained in the sieve to total weight, the fraction of fine sediments composed of silt and clay ($f_{S\&C}$) could be calculated by difference.

MASS BALANCE MODELING APPROACH

Figure 2 shows that the basic conceptual design of the TP mass-balance model applied to the Itaipu lagoon is based on the spatial model segmentation and components adapted from (Zhang et al., 2013). It is a box-model with compartments that divide the lagoon into three sedimentation zones based on their TP content: (i) the upper zone (*uz*) that receives the TP load from tributaries in an area of 0.3 km², in which the inflow is dominant and sedimentation occurs; (ii) the middle zone (*mz*), occupying an area of 0.4 km², wherein TP transport balance by tides is more important than sedimentation; and (iii) the lower zone (*lz*), which is along the tidal channel and occupies a narrow strip of 0.1 km², wherein TP exports to the sea predominate and sedimentation is negligible. The model components were calculated using actual sedimentary data as well as previous data from studies on sedimentation rates (Cerda et al., 2016), from hydrological reports about PILAS water quality (TP concentrations), and on river discharges (Niterói, 2019) in addition to measurements of nutrient fluxes along tidal cycles in the Itaipu channel, carried out between 2006 and 2007 (Marques Jr. et al., 2006). The components and budgets of the TP mass-balance model, all in Kg P.d^{-1}, are described below:

- $Settling\,(P_{set}) = SAR\,\chi\,A\,\chi\,TP_{sIL}$
- $Resuspension\,(P_{res}) = P_{ste}\,\chi\,(1-f_{s\&c})\,\chi\,R_l\big/D_s$
- $Burial\,(P_{Bur}) = P_{set} - P_{res}$

- $Inflow\,(P_{Inf}) = TP_{wRiv}\,\chi Q_{riv}$
- $Outflow\,(P_{out}) = TP_{wIL}\,\chi\,Q_{riv}$
- $Ebbflow\,(P_{Ebb}) = TP_{wIL}\,or\,TP_{wCh}\,\chi\,Q_{EBB}$
- $Floodflow\,(P_{Flood}) = TP_{wIL}\,or\,TP_{wCh}\,\chi\,Q_{Flood}$

Budgets:

- $P_{Bud}^{uz} = P_{inf} - (P_{out} + P_{Bur}); P_{Bud}^{mz} =$

$(P_{out} + P_{Flood}) - (P_{Ebb} + P_{Bur}); P_{Bud}^{lz} = $

$P_{Flood} - (P_{Ebb} + P_{Bur})$

- $P_{Bud} > 0 = TP\,Import; P_{Bud} < 0 = TP$

Export; $P_{Bud} = 0\,means\,TP\,balance$

SAR is Sediment Accumulation Rate, A is zone area, $f_{S\&C}$ is silt and clay fraction, D_S is sample depth, and R_l is roughness length, following the classification proposed by (Abbot & Basco, 1989). This parameter controls bottom friction according to sediment type (Table 1), which means that the longer the roughness and the lower the water column depth, the greater the tidal energy dissipation at the bottom, which increases the resuspended fraction. Conversely, fine particles have a shorter roughness length, leading to low bottom friction and thus lower resuspension by tides.

Q_{riv}, Q_{ebb}, and Q_{flood} are discharge ranges of rivers, ebb, and flood tides, respectively. TP_{wRiv}, TP_{wIL}, and TP_{wCh} are TP concentration ranges in waters of rivers, Itaipu lagoon, and tidal channel, respectively. TP_{sIL} is the TP concentration range in lagoon sediments. Table 1 compiles the range (minima and maxima) of each parameter with their respective units.
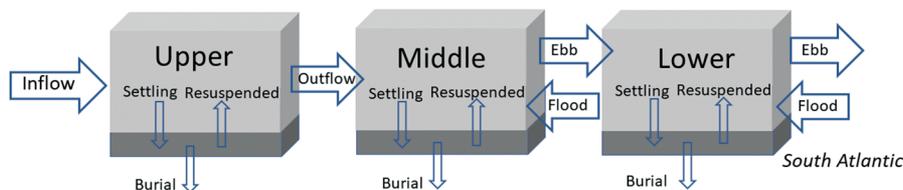

Figure 2. Schematic representation of the total phosphorus (TP) balance in the Itaipu Lagoon. Arrows indicate mass flows through the system. Light grey boxes represent the water column, while dark grey ones stand for the bottom sediments.

Table 1. Data compiled from previous and current studies, according with different time scales (wet and dry periods for TP concentrations and flows; interannual for sediment chronology) in each of the three zones used in the mass balance model, as following: Sediment Accumulation Rates (SAR) minimum and maximum values obtained from 210Pb dating cores[1]; minimum and maximum concentration of TP measured in the lagoon waters (TP_{wIL})[2], in the waters of the main tributaries (TP_{wRiv})[2], in the waters of the tidal channel (TP_{wCh})[3] and in the lagoon sediments (TP_{sIL})[4]; minimum and maximum flow of rivers (Q_{riv})[2] and tidal channel ($Q_{ebb-flow}$)[3]; minimum and maximum Inflow of TP load from rivers[2] and TP Export to the sea[3]; minimum and maximum values of the grain size silt and clay fraction ($f_{S\&C}$)[4] and Roughness length classification (R_l)[5] of lagoon sediments.

	SAR[1] $kg\ m^{-2}\ y^{-1}$	TPwIL[2] $mg\ L^{-1}$	TPwRiv[2] $mg\ L^{-1}$	TPwCh[3] $mg\ L^{-1}$	TPsIL[4] $\mu g\ g^{-1}$
Upper	2.19 - 8.76	0.16 - 0.3	0.58 - 1,34	-	814 - 1243
Middle	0,36 - 2,19	0.1 - 0.23	-	-	380 - 627
Lower	0.04 - 0.36	0.1 - 0.35	-	0,014 - 0,32	60 - 147
	Q_{riv}[2] $L\ s^{-1}$	$Q_{ebb-flood}$[3] $L\ s^{-1}$	TP Inflow[2] $Kg\ d^{-1}$	TP Export[3] $Kg\ d^{-1}$	$f_{S\&C}$ (%)[4] R_l (m)[5]
Upper	41 - 797	-	3.12 - 62.4	-	88.9 - 98.7 0.01 (pelite)
Middle	-	-	-	-	73.1 - 99.1 0.02 (pelite to fine sand)
Lower	-	4 - 39 E03[ebb] 4 - 55 E03[flood]	-	1.44 - 40.8	1.7 - 8.7 0.03 (fine sand)

[1]Cerda (2016)

[2]Niterói (2019)

[3]Alves (2007)

[4]This study

[5]Abbot and Basco(1989)

PHYSICOCHEMICAL PARAMETERS

In situ measurements were carried out in water to assess the spatial distribution of salinity, dissolved oxygen (DO), and Secchi depth (transparency) using a multiparametric probe (Hydrolab®HL7) and a Secchi disk. In addition, secondary data of the same parameters, using another multiparametric probe (HORIBA U-52G) and Secchi disk, were compiled from reports of monitoring campaigns (Niterói, 2019). These field campaigns were conducted between April 2018 and June 2019, while in situ measurements for this study were conducted between July 2019 and March 2020. The selected sampling stations were taken within the same location as the compartments used for the mass balance model (Upper, Middle, Lower). The ratio between Secchi and water depth ($R_{sec/wd}$) was calculated (varies from 0 to 1) in order to make inferences about suspended particulate matter (SPM) and light at the sediment-water interface. These data are presented as average values ± SD (number of measures) for monitoring campaigns, which were divided in accordance with wet or dry weather.

STATISTICAL ANALYSIS

Descriptive statistics (mean, range, and standard deviation) and interpolated mapping were determined for TP/IP/OP, OM, pH, Eh, fine sediments (Clay&Silt), and water depth (W_{dep}). Normality was checked by Shapiro-Wilk tests. Nonparametric correlation tests (Spearman) were applied when the assumptions of parametric tests (Pearson) could not be met with both non-transformed and transformed data, while the dependent variables (e.g. TP and IP) were not correlated.

To group sampling stations with similar characteristics in terms of sedimentary composition, a Q-mode Cluster Analysis (CA) based on Euclidean distance with z-score standardization and UPGMA (Unweighted Pair Group Method with Arithmetic mean) was applied. The groups of stations established by the Q-mode CA were then used to identify areas with different characteristics in the Itaipu lagoon. A principal components analysis (PCA) was used to summarize major patterns of variation. The PCA was performed on the correlation matrix, and the analyzed factorial axes were those that exhibited eigenvalues significantly higher than those produced by matrices of the same dimension bootstrapped 1000 times (Peres-Neto et al., 2003). The PCA results are presented in biplot format, with the variables indicated by arrows and sampling stations by points.

Statistical analyses were carried out using the R Studio software (RStudio Team, 2020). The maps were produced using Surfer® software, with coordinates according to the WGS84 (UTM-23) datum.

RESULTS

Table 2 displays the sample locations and their respective water column depths. Total, inorganic, and organic phosphorus contents (TP, IP, OP, respectively) varied between 60 and 1356 µg g^{-1} (mean 635 µg g^{-1}±348), 49 and 1194 µg g^{-1} (mean 494 µg g^{-1}±312), and 11 and 262 µg g^{-1} (mean 141 µg g^{-1} ±65), respectively. Organic Matter ranged between 0.6 and 26% (mean 16.9% ±6.4),

Table 2. Geographic coordinates, water depth and details of the studied sampling stations in Itaipu Lagoon.

Sampling points	Latitude (S)	Longitude (W)	Water depth (m)	Observations station located
LI-00	-22,967478	-43,047011	0,80	In the Itaipu tidal channel*
LI-01	-22,956028	-43,044167	1,10	Near Camboatá channel mouth
LI-02	-22,956694	-43,040833	0,80	Near João Mendes River mouth
LI-03	-22,957083	-43,038722	1,20	Near Vala river mouth
LI-04	-22,958000	-43,044972	1,50	Near west mangrove area
LI-05	-22,957722	-43,042722	1,60	From upper to middle zone
LI-06	-22,958500	-43,039583	1,50	From upper to middle zone
LI-07	-22,958472	-43,036972	1,00	Near Colibris creek mouth
LI-08	-22,960000	-43,045167	1,80	Near west mangrove area
LI-09	-22,959778	-43,042667	2,00	Middle zone of the Itaipu lagoon
LI-10	-22,960194	-43,040250	1,90	Middle zone of the Itaipu lagoon
LI-11	-22,960611	-43,037639	1,20	Near east mangrove area
LI-12	-22,961917	-43,045639	2,40	Near west mangrove area
LI-13	-22,961778	-43,043083	2,50	Middle zone of the Itaipu lagoon
LI-14	-22,962167	-43,040444	1,90	Middle zone of the Itaipu lagoon
LI-15	-22,962583	-43,037556	1,40	Near east mangrove area
LI-16	-22,963806	-43,044694	5,00	Close to tidal channel
LI-17	-22,963333	-43,042278	2,10	Transition area to tidal channel
LI-18	-22,963917	-43,039111	1,10	Near east mangrove area
LI-19	-22,965111	-43,041806	1,10	Close to tidal channel
LI-20	-22,954167	-43,045250	1,30	In the Camboatá channel
LI-21	-22,955056	-43,040500	1,50	In the João Mendes River
LI-22	-22,955500	-43,038528	0,80	In the Vala river

*Alves (2007)

pH between 6.83 and 8.12 (mean 7.73 ±0.28), Eh between -385 and -205 mV (mean -313 mV ±37), and silt and clay fraction between 1.7 and 99.3 % (mean 78.3 % ±29.6). The lagoon average depth was 1.7 m (±0.9), 70% deeper than had previously been reported (Kuchler et al., 2005), reflecting the closure of the tidal channel after a flooding event caused by high rainfall in August 2020.

SPATIAL DISTRIBUTION

The distributions of TP, IP, and OP in the Itaipu lagoon are plotted in Figure 3. OM and $f_{S\&C}$ are shown in Figure 4, while pH, Eh, and depth are shown in Figure 5. The OP distribution pattern was different than TP and IP, which were more enriched in the inner portion of the lagoon (LI-01 to LI-07). They were shown to be related to river discharges, which have IP content like river samples (LI-21 & 22), except for one single enriched station near the tide flow area (LI-17). Otherwise, OP is more ubiquitously distributed from the lower to middle zones, but at a lower concentration than IP. OM and $f_{S\&C}$ were distributed like OP, with more organic and finer sediment occupying the middle zone and mangrove areas. Redox potential (Eh) is negative in the entire lagoon. Therefore, the dissolved nutrients in interstitial waters tend to lose their electrons to new species (i.e., to be oxidized by reducing the new species). Eh and pH showed independent patterns (Figure 5) in which pH defined two fronts, one lightly acidic near the shore and another alkaline near the tributaries, i.e., pH approaches neutrality near the tidal channel (LI-16) and becomes more alkaline towards the upper zone, reaching maxima at the João Mendes river mouth (LI-2). Redox potential is less negative near the main flows into the lagoon, from both the sea (LI-16) and the João Mendes river (LI-2), whereas in mangrove areas it is more negative. Depth is greater close to the tidal channel (LI-16) and declines towards the upper zone of the lagoon (LI-2). IP enrichment in sediment was found in transition areas, from lotic to lentic environments, which occurred near the mouths of the João Mendes river (LI-2) and Colibris creek (LI-7), as well as in the middle area under the direct influence of tides (LI-17). IP enrichment is even greater in this area,

reaching 94% of TP compared to 82% and 79% in the river discharges (LI-2/3/7). OP is also found to be related to river discharges, especially from the Colibris creek (LI-7) and the Camboatá channel (LI-1), where values reached the highest percentages of TP (31% to 42 %) in mangrove areas (LI-4/8/18/19).

Only P components (TP, IP, OP) and Redox potential (Eh) showed normal or transformed-normal distributions, while pH, OM, $f_{S\&C}$, and depth failed to do so. Pearson's correlations were significant only between TP and IP/OP, which are dependent variable and, therefore, were not considered. Spearman's positive correlations were significantly high between $f_{S\&C}$ and OM content (r=0.80, p<0.05) and for OP with $f_{S\&C}$ (r=0.70, p<0.05) and OM (r=0.71, p<0.05). Negative correlations were found for depth with pH (r=-0.56, p<0.05) and Eh (r=-0.47, p<0.05), while the relationship of TP with these parameters should be seen with caution due to the significant differences between sites near the tidal channel and the others. To avoid such problems, all parameters were standardized by the z-score procedure for statistical analysis.

Salinity is quite homogeneous in all compartments with no significant differences between averages, except in the upper zone during the wet season (t-test, p<0.05). This clearly shows that the saline tide inlet is spread throughout the lagoon, while the summer rainy season is a significant freshwater source near the tributaries. Secchi depth and the ratio Secchi to water depth are also homogeneous, especially during the wet season, with similar water transparency across the lagoon reaching approximately half way through the water column. During the winter dry period, the upper and middle zones had the highest water transparency and light penetration. Conversely, the lower zone had only 20% light penetration. This means that the influence of the tidal inlet produces an unbalance condition among the three compartments during the winter. Table 3 showed oxic waters in the Itaipu lagoon, which has more oxygenated waters during the dry than the wet period, but somewhat different between the three zones. Dissolved Oxygen (DO) is lower in the upper zone, near the tributaries, but also in the middle zone during the
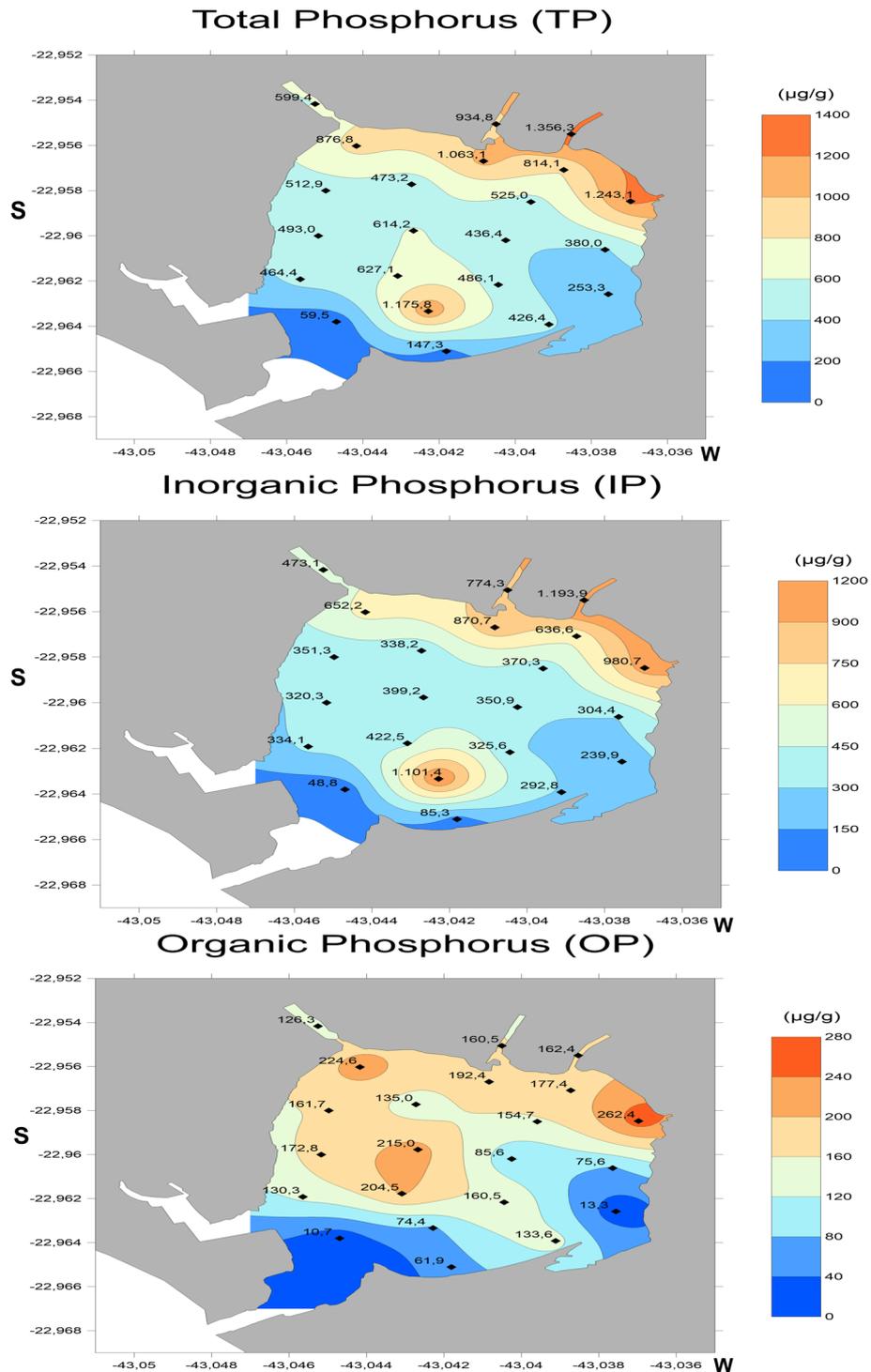
Total Phosphorus (TP)

Inorganic Phosphorus (IP)

Organic Phosphorus (OP)

Figure 3. Map of the spatial distribution of total phosphorus (TP), inorganic phosphorus (IP), and organic phosphorus (OP) concentrations (µg g-1) in the Itaipu Lagoon.

rainy period. Conversely, the lower zone always has the highest values of DO, which probably reflects the water renewal influence through the tidal inlet. (Table 3)
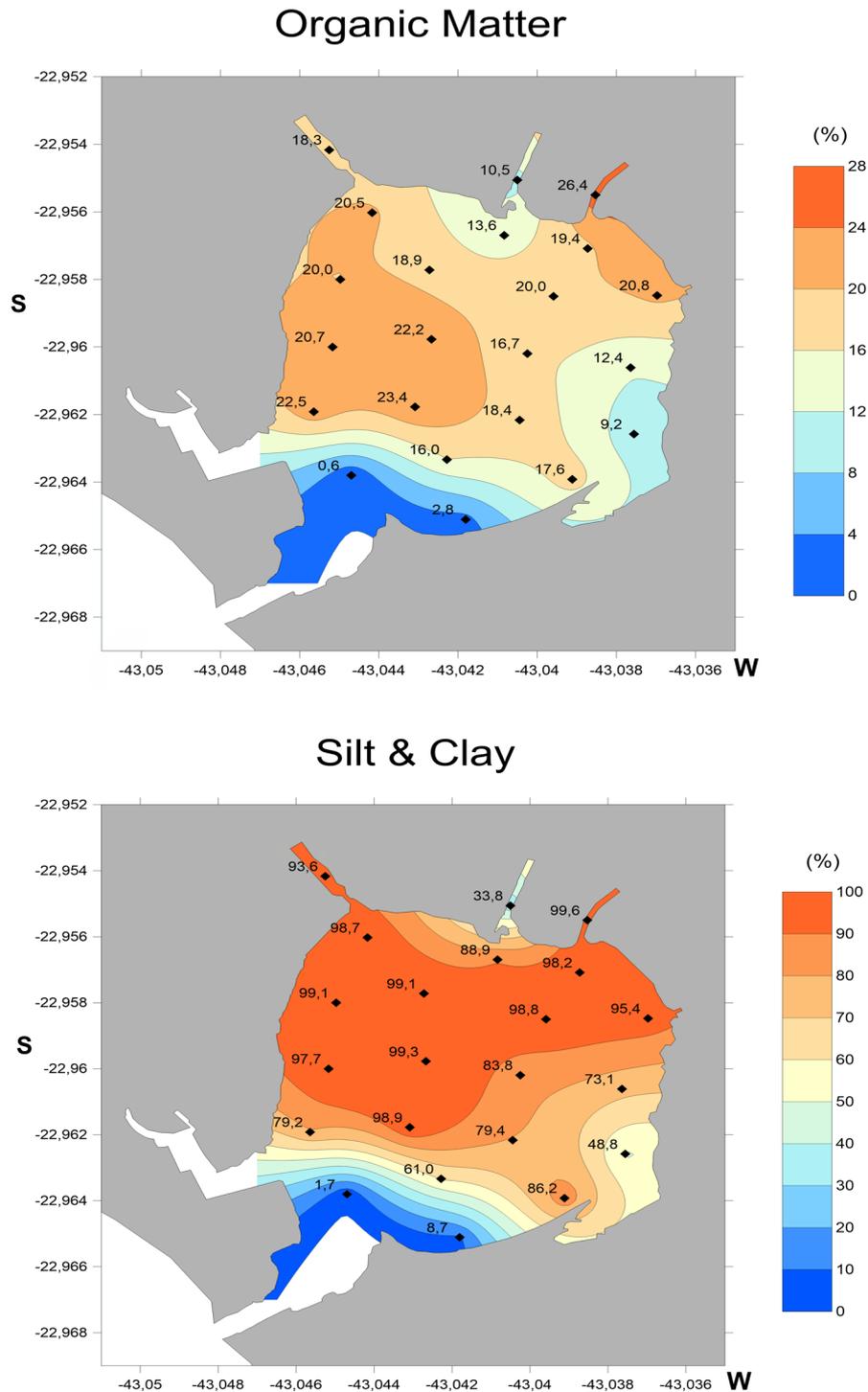
Organic Matter

Silt & Clay

Figure 4. Map of the spatial distribution of organic matter (OM) and fine sediments (fS&C) contents (%) in the Itaipu Lagoon.

SEDIMENTARY ENVIRONMENTS

Figure 6 shows a diagram of the combined effect of Eh and pH on phosphorus (P) retention in Inorganic (IP) or Organic (OP) forms. Sediment pH showed a clear distinction between two end members, one with lightly acidic conditions and
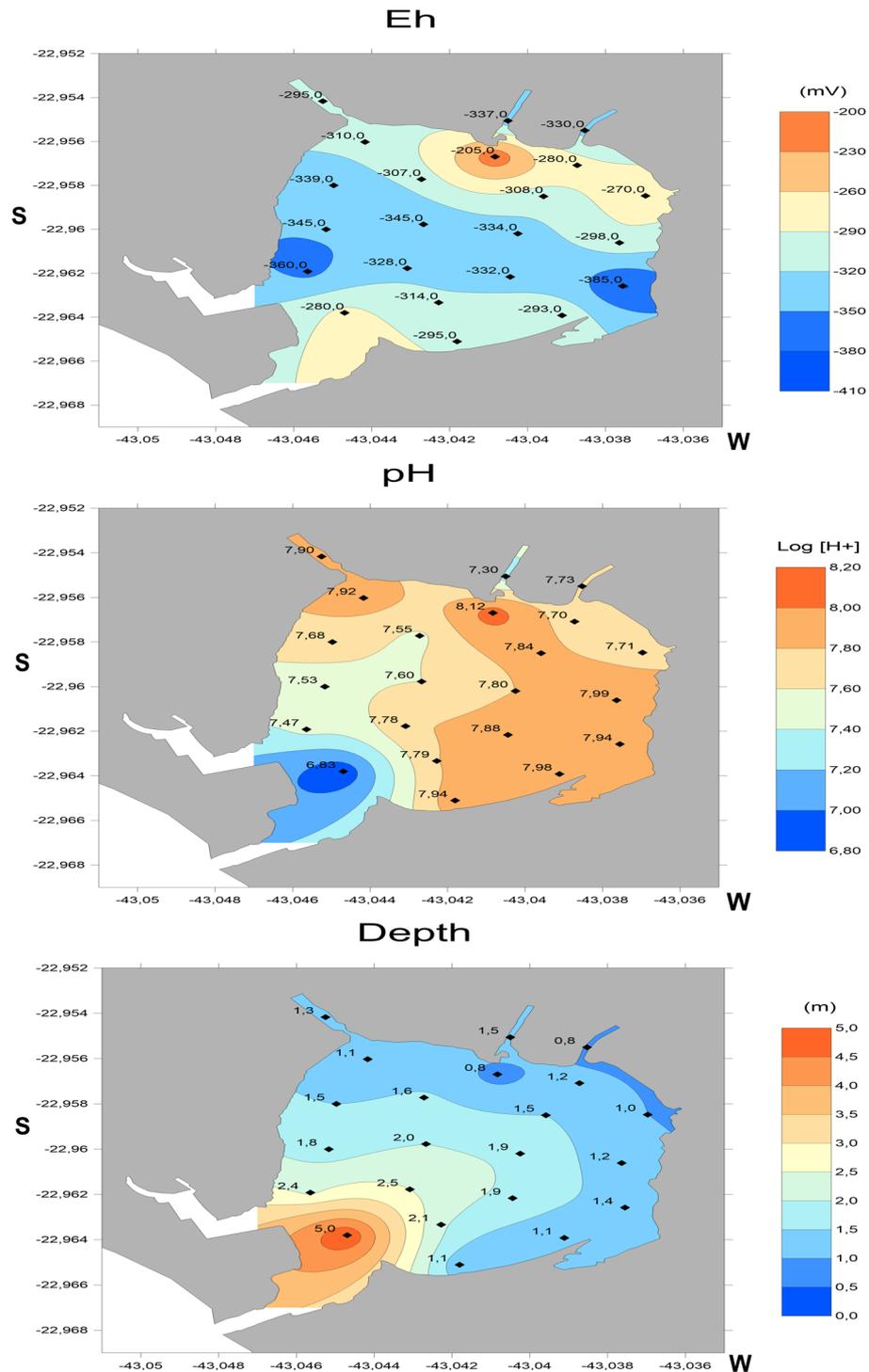
Figure 5. Map of the spatial distribution of pH (Log {H+}), Eh (mV), and depth (m) in the Itaipu Lagoon

depleted P at the tidal channel (LI-16) and another with alkaline conditions and P enrichment at the mouth of rivers (LI-2/3/7). Each of these sites have higher Eh, showing less reducing potential related

to particulate renewal, either coming from catchments or tides. Except for two sites more related to the sea (LI-16 and LI-15), all other samples align in one of two Eh-pH linear sets. The first

Table 3. Salinity, Dissolved Oxygen (DO), Secchi depth (transparency) and ratio between Secchi and water depth ($R_{sec/wd}$) were measured at three stations inside the Itaipu Lagoon, within the same location as the compartments used for the mass balance model (Upper, Middle, Lower). The data are presented as average values ± SD (number of measures) for monitoring campaigns during wet and dry weather.

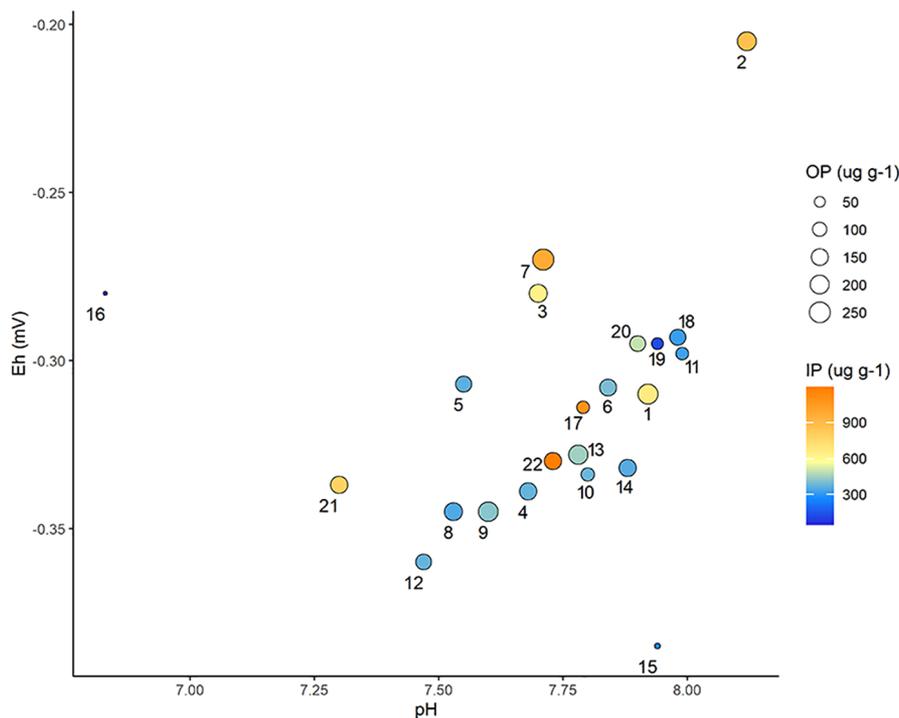| Dry Season	Salinity ‰	DO mg L^{-1}	Secchi Depth cm	$R_{sec/wd}$ (0 ~)
Upper	27.3 ± 2.5 (n=6)	6.58 ± 1.66 (n=11)	56.0 ± 28.9 (n=4)	0.53
Middle	26.8 ± 3.2 (n=6)	8.3 ± 1.23 (n=11)	61.25 ± 21.75 (n=4)	0.50
Lower	26.4 ± 3.4 (n=6)	8.37 ± 2.79 (n=11)	38.75 ± 23.23 (n=4)	0.20
Wet Season				
Upper	17.9 ± 3.1 (n=6)	6.18 ± 2.62 (n=11)	45.0 ± 10.8 (n=4)	0.51
Middle	25.5 ± 5.7 (n=6)	5.85 ± 2.29 (n=11)	41.25 ± 9.46 (n=4)	0.48
Lower	26.5 ± 5.2 (n=6)	7.09 ± 2.15 (n=11)	47.5 ± 15.55 (n=4)	0.43

Figure 6. Eh - pH diagram showing their combined effect on phosphorus in Inorganic (IP) and Organic (OP) forms.

linear set is formed by P rich-samples from the João Mendes river (LI-21: less alkaline and reducing potential) to its mouth (LI-2: more alkaline and less reducing potential), including nearby samples in the lower region, which received a contribution from tributaries (LI-3/5/7). The second linear set comprises all remaining samples (LIs-1/4/6/8/9/10/11/12/13/14/17/19/20/22) that do not show a clear trend, with both enriched and depleted P mixed along the line. Thus, we can divide the

lagoon into a lower zone connected to the sea, an upper zone receiving the contribution of the PILAS sub-basins, and a middle zone of the mix line.

Results of Q-mode CA, based on all parameters, indicate three main clusters of stations (Figure 7). Cluster 1 can be further subdivided into two subsets of stations, the first (1.1) formed only by the sample in the tidal channel (LI-16), while the second (1.2) containing stations that probably receive contributions from the salt wedge (LI-15 and LI-19). Cluster 2 is formed by a cascade of smaller groups with no meaning other than representing the mixing process from the inner portion towards the center of the lagoon. Cluster 3 represents the continental component and is subdivided into two subsets, the first (3.1) formed by transition zones between the João Mendes river and Itaipu lagoon (LI-21) and between the continental and tides flows (LI-17), while the second (3.2) comprised of areas that receive the discharge at the mouths of João Mendes, Colibris, and Vala rivers (respectively, LI-2, LI-7, and LI-22). CA cophenetic correlation coefficient, which is a measure of reliability between the UPGMA method clustering and similarity matrix of standardized objects, was 0.908, considered significant (R Core Team, 2020).

Results showed that cluster 1 was deeper (2.5 m ± 2.2), less alkaline pH (7.37 ±0.5), and sandy

(80.3% ± 17%) with low P (TP = 153 µg g^{-1} ± 97) and organic matter (4.2% ± 4.5) content. Cluster 2 was characterized by the highest $f_{S\&C}$ (90 % ± 10%) and OM (19.1% ± 2.8%) and intermediate P content (TP= 594 µg g^{-1} ± 212) and depth (1.7 m ± 0.5). Cluster 3 had the highest P content (TP= 1155 µg g^{-1} ± 162), with more alkaline (pH= 7.83 ± 0.3) and less reducing (Eh = -291mV ± 55) sediment in the shallowest part of the lagoon (1.2 m ± 0.6).

The PCA biplot (Figure 8), which explains most of the data variability (68%), had the same cluster groups as Figure 7. Except for redox potential (Eh), all variables were plotted on the first axis (PC1≈50 %), while depth was in opposition to TP, IP, and pH. The samples related to the tidal channel and salt wedge are associated with higher depth, while the samples receiving a riverine discharge (João Mendes, Vala, Colibris) are associated with higher TP, IP, OP, and pH. Conversely, most of the samples are grouped in the middle of the two axes and represent, in Euclidean space, the mixing line in Figure 6, which is generally related to high $f_{S\&C}$ and OM. The transition subgroup is graphically represented between the discharge and mixing groups and may be related to specific redox and pH conditions for adsorption, leading to unexpected P contents in sediments.
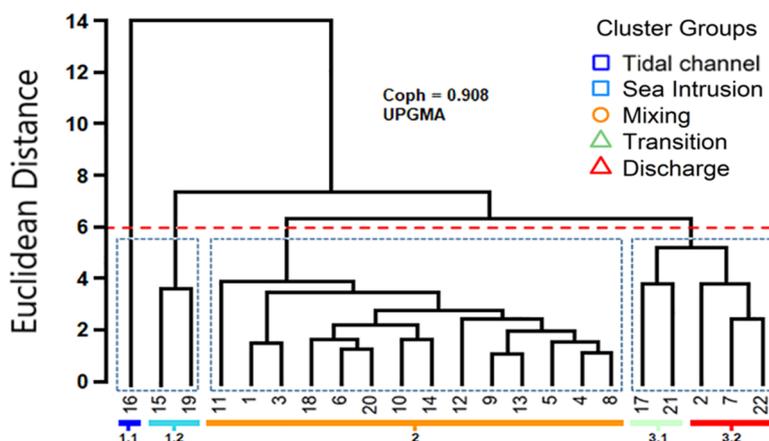

Figure 7. Dendrogram showing the three main cluster groups: i) tidal channel and salt wedge; ii) mixing line from banks to center, iii) discharges and transition areas.
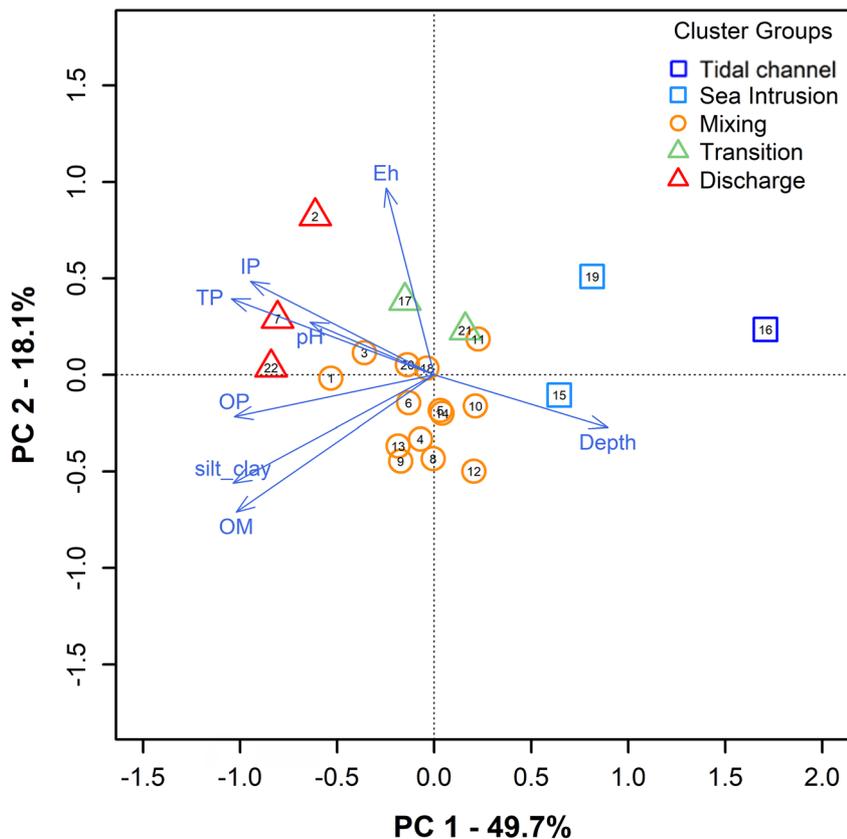
Figure 8. Principal Component Analysis biplot showing the same cluster groups of samples and relationship among parameters.

MASS BALANCE

All TP components and budgets were quantified for each zone during dry and wet seasons (Figure 9), according to the mass balance box-model (see in methods). TP was added to sediment through a settling process (P_{set}), occurring mostly in the upper zone where it reaches 7.2 ($\pm$ 1.44) and 1.68 ($\pm$ 0.24) Kg P d^{-1} during wet and dry seasons, respectively. P_{set} is up to one order of magnitude smaller in the middle zone (1.2 $\pm$ 0.24 and 0.19 $\pm$ 0.05 Kg P d^{-1} for wet and dry seasons, respectively) and up to three orders of magnitude smaller in the lower zone (0.0144 $\pm$ 0.007 and 0.001 $\pm$ 0.000192 Kg P d^{-1} for wet and dry seasons, respectively). Thus, in the lower zone, P_{set} can be considered negligible. TP resuspended from sediments to the water column (P_{res}) is based on constraints in P_{set} by grain size, surface roughness, and water depth. In other words, the smaller the

grain size and ratio between surface roughness and sampling station depth ($R_I/_{D_S}$), the smaller the resuspension, while P_{set} enhances oppositely (large grain size and high $R_I/_{D_S}$). P_{res} represents only 6% to 7% of the P_{set} in the upper zone and is even smaller in the middle zone (4% to 5% of P_{set}), but it can reach 58% to 70% in the lower zone. However, in all cases, P_{res} showed small figures, with the highest value of 0.48 $\pm$ 0.43 Kg P d^{-1} in the upper zone during the wet season and a smallest of 0.62 $\pm$ 0.43 g P d^{-1} in the lower zone during the dry season. Therefore, TP burial (P_{Bur}) matches most of the P_{set} in the upper and middle zones, but is insignificant in the lower zone (Figure 9).

TP inflow (P_{Inf}) from tributaries to the upper zone showed a marked seasonal variation, with the highest values (62.4 $\pm$ 33.6 Kg P d^{-1}) during the rainy period but similar to P_{set} during the dry season (4.8 $\pm$ 1.44 Kg P d^{-1}). TP outflow (P_{Out}) from the
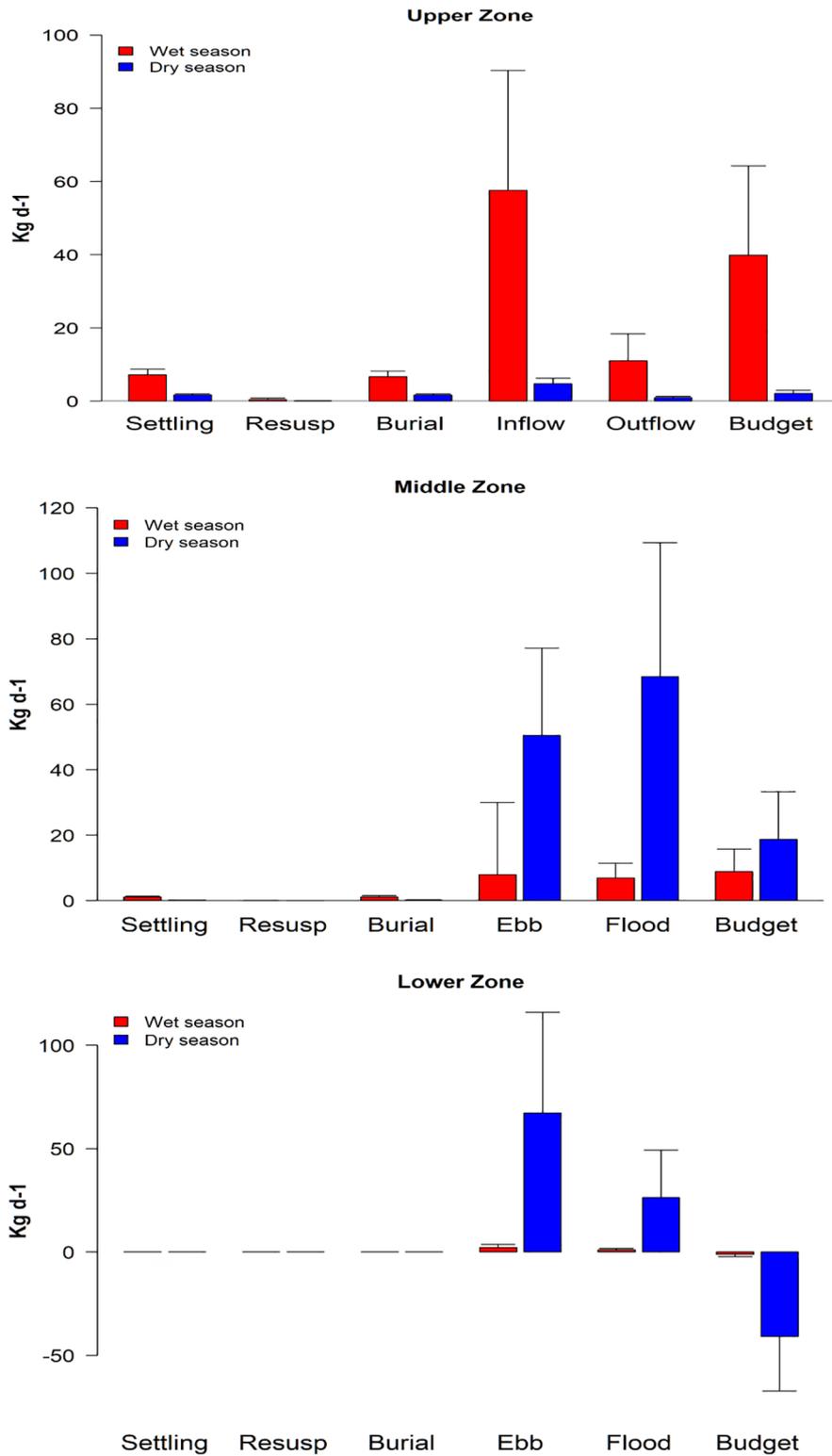
Figure 9. TP components and budgets, with their respective standard deviations, quantified for each zone in the Itaipu Lagoon during dry and wet seasons.

upper to middle zones also showed a seasonal difference, varying from 11.0 (± 7.44) to 0.96 (± 0.24) Kg P d^{-1}, during wet and dry periods, respectively (Figure 9). Tide flow is represented by flood and ebb components and is significant for TP exchanges between the middle and lower zones as well as between the lower zone and the sea, through the tidal channel. When comparing the upper zone, the first difference is a higher tide flow during the dry season (68.4 ± 41.04 and 50.4 ± 26.4 Kg P d^{-1} for flood and ebb tides, respectively) than during the rainy season (6.96 ± 4.56 and 7.92 ± 4.32 Kg P d^{-1} flood and ebb tides, respectively), caused by the entry of cold winter fronts (Kjerfve et al., 1997). This was evident from flood flows (P_{Flood}) higher than ebb flows (P_{Ebb}) transported to the lower zone only during the winter, although this TP was not being buried in lower or middle zones. This question will be addressed in the following discussion.

Otherwise, tidal flow through the tidal channel, despite having similar enrichment to the middle zone during the dry period compared to the rainy season (Figure 9), had higher values during winter ebb tides (67.2 ± 50.4 and 2.16 ± 1.68 Kg P d^{-1} during dry and wet seasons, respectively) than those of flood tides (26.4 ± 22.8 and 0.96 ± 0.72 Kg P d^{-1} during dry and wet seasons, respectively). This represents net loads (total import-export balance of each tidal cycle) through the sum of partial (hourly) loads measured during the cycles. Finally, TP budget can be summarized for each zone: (i) upper zone in which the rainy season provides an increase in TP inflow, outflow, and burial, with the predominance of the former, acting as the largest import zone during the wet summer (P_{Bud}^{uz} 40.8 ± 24 Kg P d^{-1}) but having only a modest budget (P_{Bud}^{uz} 2.4 ± 0.72 Kg P d^{-1}) during the winter dry season; (ii) middle zone showing an opposite trend, with the dry winter period (P_{Bud}^{uz} 19.2 ± 14.4 Kg P d^{-1}) having twice the budget of the wet season (P_{Bud}^{uz} 9.6 ± 7.2 Kg P d^{-1}), still acting as an import area but with less significance for the burial compartment; and (iii) lower zone showing a budget dominated by TP export to the ocean, which was much higher during the winter dry season (P_{Bud}^{uz} 40.8 ± 26.4 Kg P d^{-1}) than the wet summer (P_{Bud}^{uz} 1.2 ± 0.96 Kg P d^{-1}).

DISCUSSION

Human interventions in the Itaipu lagoon system have caused a strong imbalance in biogeochemical cycles over the past decades. The resulting eutrophication has led to a change from meso- to hypertrophic conditions (Cerda et al 2013), although P loads are not particularly high compared to other eutrophic coastal lagoon systems. Factors related to the spatial distribution of P, the main sources that control the mass balance, and their effects on eutrophication are discussed below.

WHAT FACTORS CONTROL PHOSPHORUS SEDIMENTATION?

The Phosphorus dynamics in shallow coastal waters is characterized by a fast orthophosphate transformation, both through biological uptake and geochemical speciation. The orthophosphate tends to adsorb suspended material, mostly fine particles, which are often maintained at low concentrations in dissolved form, especially under high SPM concentrations (Carmouze, 1994; Conley et al., 1995; Deborde et al., 2007). A prior study (Barboza, 2003) showed high inorganic phosphorus concentrations in the seston of the Itaipu lagoon, suggesting high IP uptake by phytoplankton. However, since the geochemical speciation of phosphorus was not evaluated in this study, it is not possible to assess the significance of each process.

Cotovicz Junior et al., (2014) studied P spatial distribution in surface estuarine sediment in the Guaratuba bay (Paraná state, Southern Brazil). The authors observed a pattern somewhat similar to that in the Itaipu lagoon and found higher TP and IP values in the upper sector and transition zones between the upper and central zones. These sectors were formed by fine sediment in low-salinity shallow waters, while the lower sector and its narrow tidal channel exhibited a larger fraction of sandy sediment with lower TP, IP, and OP content. However, the authors also reported TP, IP, and OP concentrations much lower than those in the Itaipu lagoon, especially in the upper zone where IP was less than one third (240 µg g^{-1} vs. 850 µg g^{-1}) and OP less than half (95 µg g^{-1} vs.

195 µg g^{-1}). This is because the Guaratuba bay is a semi-pristine habitat compared to the Itaipu lagoon, which features higher urban density and more engineering interventions, thus reinforcing its hypertrophic state due to sanitation inefficiency and water treatment by the sewage company. Another difference concerns water salinity, quite homogeneous in the Itaipu lagoon, at least during the dry season, while constant and low in the upper compartment of the Guaratuba bay. This can be explained by the small size in relation to the tidal prism of the prior compared to the latter, whose upper zone is located far from the sea channel and is controlled by larger rivers.

Sedimentary P can occur in the form of precipitates (Ca, Fe, or Al) or adsorbed onto the surface of Fe/Al minerals. Despite controlling P mobilization through iron binding in lake sediment (Heinrich et al., 2021), Fe(III)-bound phosphate can dissolve inside reduced zones (Andrieux-Loyer & Aminot, 2001). Phosphate desorption associated with pH and Eh gradients often leads to a decrease in sedimentary P from the upper to the lower intertidal estuarine zones and increases eutrophication (Andrieux-Loyer et al., 2008; Gao et al., 2012). We did not measure Fe/Al concentration or assess phosphate speciation. However, the Eh-pH diagram shows some clear pathways for P sedimentation. High IP values are mostly related to pH above 7.5, regardless of the reducing conditions, while the lowest one is related to lightly acidic pH (< 7.0). The relationship between increase in pH and IP, which can be seen in the PCA biplot (Figure 8), is probably caused by Ca-P mineral formation. It switches from P adsorption to precipitation of Ca-P and decreases phosphate solubility (Oxmann & Schwendenmann, 2015), even inside reduced zones. In general, nutrient uptake during photosynthesis is related to pH increase due to CO_2 consumption (Soetaert et al., 2007). Photosynthetic activity takes place on the water surface and is unlikely to occur at the sediment-water interface, as the water transparency values are always a fraction of the depth of the water column (Table 3).

The lagoon hydrodynamic circulation is relatively homogeneous, as shown by the salinity data (Table 3), except during the rainy summer, when the increase in river discharge caused salt dilution in the upper zone, forming a freshwater front that reduces penetration from the saline wedge. The circulation of seawater along the lagoon through the tidal channel, where high DIC concentrations and alkaline pH were found (Marques Jr et al., 2006), probably contributes to precipitation of a thin marine calcium carbonate layer on surface sediment. The formation of Ca-P in sediment, as discussed above, is likely related to such a marine source, which contributes to mitigating P-related eutrophication. Conversely, the slightly acidic pH and P depletion near the tidal channel is controversial, but two possible and complementary explanations could be: i) the settling of fine particles, as shown in mass balance (see results section and Figure 9) is negligible at this deeper tide-dominated site, which means there is less marine carbonates on the bottom; and ii) Al/Fe-P bond predominates at this lower pH, and its dissolution occurs in reducing sediments. It is noteworthy that this site also provided the lowest values of TP, IP, OP, OM, and $f_{S\&C}$.

The highest IP concentrations were found in the Vala river (LI-22) and near the mouths of the Colibris (LI-07) and João Mendes (LI-02) rivers, forming P burial spots which are possibly related to Ca-P precipitation, as previously discussed. Furthermore, this process may influence the high IP concentration found in the transition to the tidal channel (LI-17), which would take place under same pH range (> 7.7). The possible causes for such values at a location far from the rivers are discussed in the next section. When compared to other tributaries, João Mendes river is dominated by sand grains and has a lower OM content and pH. This is probably related to erosion in this basin since the last decade. This process accelerated after a large landslide in an urban settlement in the city of Niterói, caused by a tropical storm event in 2010 (Morro do Bumba). According to IPCC reports, landslides and flood events have been more frequent in the last decades due to climatic drivers, which could accelerate river siltation and turbidity, changing the Itaipu lagoon to a heterotrophic state.

In short, IP enriched sites are influenced by discharges of tributaries and related to the transition

zone to the tidal channel. Conversely, OP could be recycled through enzymatic hydrolysis by microorganisms (algae, bacteria, and zooplankton), allowing P retained in organic particulate form to become available for uptake by phytoplankton and be incorporated into the biomass. Extracellular phosphatases are particularly important in this process, because they catalyze the hydrolysis of organic phosphorus compounds to inorganic phosphate (Panosso, 2001). As mentioned here, phosphate fluxes were found from sediment in eutrophic environments, even in oxygenated waters. As such, it is reasonable to assume that this process is occurring in the Itaipu lagoon and may be connected with the lower concentration of OP in sediment. In a biogeochemical study carried out in a eutrophic embayment, Markovic et al. (2019) found that even in well-oxygenated waters, diffusive P fluxes from sediment of short duration occurred. The authors concluded that OP mineralization in anoxic sediment is the main contributor to internal P loading, which is coupled with redox-sensitive Fe cycling.

Two other possible reasons for the low concentrations of OP in the lagoon sediment are: i) TP loads are mainly composed of inorganic forms (e.g., detergents, phosphogypsum-based building material, detrital apatite from rock weathering) with fewer OP sources; and ii) it is mostly exported to sea in suspended particulate material or as Colloidal Organic Phosphorus (COP) produced by phytoplankton and remineralization during downward transportation in the water column (Cai & Guo, 2009). It would be ideal to address each issue, such as monitoring OP loads and orthophosphate in rivers, lagoons, and inlets, in addition to treated and untreated domestic effluents, and to search for the presence of phosphogypsum in building materials. However, this is outside the scope of the present study.

Regarding spatial distribution, OP has the same source as IP but a different fate. The highest OP concentrations are in stations near the main discharges (Colibris, João Mendes, and Vala) and the center of the Itaipu lagoon, while the lowest are near the connection with the sea and in areas affected by the saline wedge. Such a condition is corroborated by the significant positive correlations of OP with OM and $f_{S\&C}$. Furthermore, when considering the contribution of the OP fraction to TP, the highest percentages are found not only in the middle zone but also in mangrove areas, where they reach a maximum contribution (42%). In general, low salinity areas are highly heterotrophic and oxygen-depleted, in addition to acting as strong CO_2 sources for the atmosphere (Frankignoulle et al., 1998), whereas at high salinity, phytoplankton can grow and produce a significant atmospheric CO_2 sink (Borges and Abril, 2011). The heterotrophic condition should prevail only in watercourses with slow residence times, lower DO, and salinity, such as the Camboatá channel (see next section) or during short rainy periods. The degree of heterotrophy must be mainly related to OM accumulation from freshwater discharges in the upper and middle zones, which probably explains the greater OP contribution to the phosphorus budget. Recent studies in tropical estuaries have reported different CO_2 flux patterns, with an atmospheric CO_2 sink induced by eutrophication (Cotovicz et al., 2015, 2020).

On the other hand, the OP has a higher contribution in mangrove areas, which could be related to its mobilization in sediment as Fe-bound phosphate found in the rhizosphere (Jian et al., 2017). However, the relationship between OP and DO remains unclear, especially in terms of the differences observed between the western and eastern areas. The west side, situated in a larger mangrove patch, receives loads from upstream rivers and has higher OP, OM, and $f_{S\&C}$ content. It is located between the upper and middle zone, where lower DO values probably relate to discharges of organic loads from tributaries. The east side has lower OP, OM, and $f_{S\&C}$, occupying a narrow fringe of mangrove in the middle zone and receiving waters from both the tidal channel and rivers during the wet season. This balance contributes to an oxic state throughout the year by tidal input, though the DO decrease in the middle zone during the wet period suggests the extent of eutrophication consequences in the center of the lagoon, where OP content is high. The very low OP content observed in station LI-15 is probably related to the dominance of sand grains and the east mangrove havoc (occupied by dwellings), which has a smaller structure without a well-developed rhizosphere.

The above-mentioned patterns become more clear through the Cluster Groups. In Group 1, for instance, P input into the Itaipu lagoon was not largely influenced by tides, which seem to have exported it to sea instead (see next section). Group 2 represents the mixing line also observed in the Eh-pH diagram. This line shows that P tends to accumulate from the banks towards the center of the lagoon and in some mangroves. There, OM and $f_{S\&C}$ content are significantly correlated with OP, as also observed in the PCA biplot. Finally, Group 3 includes P-enriched stations in the upper zone and rivers, as well as between the middle zone and tides, suggesting these areas are spots for P burial, especially for IP. The opposition of TP and IP to depth in the PCA biplot seems to show the relation of P source to river inflow producing siltation and nutrient enrichment. These features lead to shallower sedimentary environments, which is related with soil weathering and erosion. On the other hand, the opposition of pH to depth seems to be biased by the lowest value of the deeper site near the tidal channel, as discussed earlier. The PCA's first axis seems to explain the origin of P according to its source proximities, while the second axis is driven only by redox potential (Eh), which explains much less of the data variability and seems to be unrelated to P distribution.

The present study aimed to add information on the role of P in eutrophication by quantifying TP loads from basins as well as TP balance in the tidal channel. These findings are discussed in the next section.

What are the sources controlling the TP budget and their effect on eutrophication?

Prior studies have addressed historical changes in the P flux of coastal lagoons on the east coast of Rio de Janeiro state (Brazil). According to these reports, P input has increased since the 1970s, which marks a land use change towards the growth of urban settlements in the region, with sharp rise over the last 20 years (Galvão, 2008). P inflow has a positive and significant relationship with population census growth in sub-basins (Cerda et al., 2016). Likewise, Harris (2001) found that TP flows grow exponentially in Australian urban catchments as population density increases. These findings can also be supported by comparing TP loads from rivers to the Itaipu lagoon evaluated by Knoppers et al (1991) with TP inflow in the upper zone (Figure 9) from our study. One can note that, over these three decades, TP loads increased from 33.6 to 62.4 Kg P d^{-1} in the Itaipu lagoon. Knoppers et al. (1991) classified the Itaipu lagoon as mesotrophic, which might have been due to the opening of the tidal channel in the 80s. However, it changed to a hypertrophic state after 30 years of basin intensive occupation (Cerda et al. 2013). Nevertheless, these figures are not particularly noteworthy if compared to other coastal lagoons. For instance, the evaluation of TP riverine loads delivered to the Great Barrier Reef lagoon in 14 basins of Australia showed mean values of 225.6 Kg P d^{-1} (19.2 to 1,068) and 703.2 Kg P d^{-1} (88.8 to 3,014.4) for pre-European and anthropogenic loads, respectively (Kroon et al., 2012). These averages are up to one order of magnitude higher than the Itaipu inflow. Kroon et al. (2012) concluded that overall TP loads rose by 8.9 times to 16,000 t y^{-1} due to land-based run-off of nutrients occurring since European settlement. However, although the great barrier ecosystems are vulnerable to eutrophication related to P loads, trophic status ranges from mesotrophic to eutrophic without approaching the tipping point for a hypertrophic condition (Sorokin & Sorokin, 2010). This is probably due to the seawater renewal caused by the larger area extension and tidal prism, limiting algal bloom debris accumulation and hence eutrophication. In the tiny Itaipu lagoon, eutrophication is favored by the accumulation of organic matter and nutrients from elsewhere in the basin, which has increased due a recent increase in water residence time. This process is likely to amplify the nutrient impact on algal blooms, changing the trophic state as algal debris accumulation increases.

Páez-Osuna et al., (2013) investigated the effect of nearby nutrient loads on algal blooms in coastal lagoons of the southeastern Gulf of California. Their results point to shrimp farms as the main point sources of P loads to the lagoons, while sewage and upwelling were suggested as significant diffuse sources. The authors also showed that nitrogen and phosphorus loads could

explain, through multivariate factor analysis, a large part of the variation in annual phytoplankton and macroalgae biomasses. Just like in the Great Barrier Reef, coastal lagoons in the Gulf of California have TP loads higher than those in our study, with an average of 170.4 Kg P d^{-1} (38.4 to 386.4). This may be because mariculture is a major additional point source of P derived from shrimp farm waste. In a study on nutrient exports in catchments in Uruguay Rodríguez-Gallego et al. (2017), the authors evaluated land-use effects on eutrophication of coastal lagoons and concluded that catchment size is inversely related to most eutrophication indicators, which is consistent with our findings discussed above. These authors also showed that larger TP loads were associated with grasslands and human settlements at least since the 1970s, and recently with artificial prairies and over-sowed areas. The TP loads from four Uruguayan coastal lagoons still connected with the sea range from 38.4 to 232.8 Kg P d^{-1}, with an average value of 115.2 Kg P d^{-1}, twice the mean value of the Itaipu lagoon.

The Itaipu lagoon is in an urban environment and does not receive P inputs from farms, grasslands, or pastures. Upwelling input occurs only during short events, with domestic sewage being the most significant source. Conversely, our budget results (Figure 9) showed the lagoon acting as a TP exporter, especially during winter (dry season), as opposed to TP inflow by rivers, which is much higher in summer (wet season). (Marques Jr, et al. 2006) showed that the primary production (Chlorophyll-a) in the tidal channel decreases during the winter, reflecting the increase of suspended particulate matter (see Secchi depth data in table 3), brought by more active tides as well as increased cloud cover. Both factors reduce solar radiation penetration and, hence, photosynthesis. In the case of suspended particulate matter, this is supported by our data, which showed much lower transparency during the winter, with only 20% light penetration (Table 3). TP exports occurred during the winter, when phytoplankton uptake probably decreased. However, the author found high chlorophyll-a concentrations, with net exports during both seasons, indicating high overall phytoplankton productivity in the Itaipu lagoon and suggesting it as a hypertrophic system, as indicated by the occurrence of diatom bloom events during summer. Finally, the author suggests that the Itaipu lagoon is an important breeding ground for fish eggs and larval forms of other organisms, mainly crustaceans, contributing to marine fishery productivity.

For management decisions, mass-balance modelling is, even in a simple form, a forecasting method of future TP concentrations for different scenarios. To perform this task, a model is built from a series of temporal data to calibrate simulations, from which the results must reproduce the variability observed in the same time interval. In a subsequent and decisive step, the model's predictive capacity is tested by reproducing other data series for validation. Such an approach involves extensive monitoring to provide evidence for decision makers. However, this depends on a long-term effort to sample, analyse, and measure water flux at various stations within the basin of the lagoon (Meals et al 2008, Zhang et al 2013). This exceeds the scope of our study, in which only short data series and a few monitoring stations are available. Thus, a mass-balance was used only to derive numbers and compare loading values between different sectors in the lagoon with other studies, as well as to identify potential divergences with sedimentary data. Our first objective was addressed in the discussion above and rendered several reasonable figures. The second will be discussed below.

Flood flow (P_{Flood}) values are higher than ebb flow (P_{Ebb}) values between the lower and middle zones during the winter season. However, a single spot with high TP concentration can be highlighted in sediment of the transition area to the tidal channel (LI-17), which was not computed in mass balance calculations, as well as the tributaries. Since this flood-ebb difference is not settled in the sediments of the lower or middle zone, which is composed by IP and very poor in OP, it suggests a possible source for LI-17 enrichment. Though it is not possible to assign a reason for this feature, it is probably a winter-related event, as it was identified during a winter sampling campaign, when

the debris from stronger tidal currents constrained photosynthesis and increased TP export to the ocean. Further research addressing P dissolved forms and their speciation, either in water column or in interstitial waters, is needed to address this question, reinforcing the importance of proceeding with this investigation.

The erosion in the João Mendes river basin might be influenced by landslides events but is also related to urban occupation since the 1970s, as mentioned above. This period was marked by the completion of public works, notably the President 'Costa e Silva' bridge, which connects the cities of Rio de Janeiro and Niterói, and the tunnel that connects the districts of Icaraí and São Francisco in Niterói. This led to a first migratory flow to the shore region of Niterói. The Ewerton Xavier avenue (formerly Avenida Central) that connected the Itaipu district to Amaral Peixoto road was built in the early 1980s. This road gives the municipalities on the east coast access to the Niterói shore region, which also contributed to urban expansion in the João Mendes river basin (Niterói, 2002). This occupation continued over the subsequent 40 years, intensively replacing vegetation cover with urban area in the João Mendes river basin (Alves et al., 2021).

There is evidence that residents of the João Mendes river basin conducted various canalizations in many 2nd and 3rd order channels. Furthermore, there are cartographic records that show that the main channel of the João Mendes river was diverted in the early 1980s (Galvão, 2008). This intervention led to the conversion of the floodplain into landfill areas, enabling various real estate developments. Another important work was the canalization in the lower course of the João Mendes river in the early 2000s, where a 148 m stretch of the river's cross section was concreted in a U shape by EMUSA (Niteroi's municipal housing, urbanization, and sanitation authority) to prevent the collapse of houses. As such, the drainage of the João Mendes river sub-basins is currently highly mischaracterized due to urban expansion. Many stretches have been diverted and/or rectified, others were filled to allow for construction, and a large part of the riparian forest that protected

the banks against erosion was removed. There is also evidence today of the decrease in flooded area on the inner edge of the Itaipu lagoon due to strong silting from sediment brought by the João Mendes river (de Azevedo, 1987; Galvão, 2008). These interventions led to an increase in hydraulic energy, allowing for greater sediment transport capacity along the João Mendes river. The synergy between landslides, river channelings, vegetation removal, and demographic growth over the last few decades has produced an increase in TP inflow, accelerating P settling. This altered the P spatial distribution in surface sediment due to biogeochemical changes in the sedimentary environment.

Though there is no inflow data available for discharge from the Camboatá channel into the Itaipu lagoon, water flows are supposed to be low and intermittent. The Camboatá channel is a narrow and shallow watercourse, where tidal currents were not expected to be significant. These features led to lower salinity ($\approx$ 18 ‰) and DO ($\approx$ 3 mg L^{-1}), according to a recent monitoring report (Niterói, 2019). However, this pattern has seemed to undergo strong changes, at least during spring tides, since the opening of the Tibau tunnel (2008) connecting the sea to the Piratininga lagoon, bringing sediment from the lagoon and its basin to the Itaipu lagoon through the Camboatá channel. This led to extra loads of P to the Itaipu lagoon, settling mainly in the upper zone, derived from continental sources discharged by rivers in the Piratininga lagoon. Such P enrichment can be observed in the upper zone of the mass balance model.

On the other hand, the permanent opening of the tidal channel (Itaipu channel) provided for the renewal of the Itaipu water. It was inversely related to most eutrophication indicators, such as nutrient loads, although it has led to shallower depths in the lower zone due to sand infill. This suggests that tidal channel management is a critical issue for maintaining ecosystems services provided by coastal lagoons. Finally, the sewage treatment plant has the potential to reduce TP loads, but only if its capacity is

adjusted meet population growth. After becoming operational in 2004, the plant appears to have made no noticeable difference (Cerda et al, 2016), but the recent doubling of its capacity may begin to have an effect on TP inflow if population growth stabilizes.

CONCLUSION

Eutrophication is a dynamic process occurring at different ecosystem states in which sedimentary phosphorus can be used as an indicator. However, this study showed that P load and burial rates in sedimentary environments *per se* are not enough to indicate the trophic state. Other features, such as residence time, tidal prism, P speciation on the water column and interstitial water, contents of organic matter and other nutrients, and extension and occupation of the basin play major roles on the impact of phosphorus loads on eutrophication. Over the past decades, the Itaipu lagoon has undergone strong eutrophication, which has been reinforced by erosion from due to historical landslides and floods. These events have accelerated siltation in the lagoon with the accumulation of nutrients and organic matter, probably leading to sediment anoxia. Furthermore, remineralization of nutrients in the water column seems to be a dominant process, suggested by the low OP values in sediments. This process contributed to export P and phytoplankton-derived organic matter to the ocean. These inputs from the catchment changed the trophic state of the lagoon from meso- to hypertrophic, as well as its morphometric and hydrological characteristics. Our findings confirm that human interventions impact nutrient loads which, in turn, disrupt the balance of biogeochemical cycling, compromising coastal water resources. Such an imbalance may collapse ecosystem services and contribute to break our planetary boundaries. Further studies involving P speciation, dissolved nutrients, particulate organic matter, and carbonate system fluxes are needed to better understand the current trophic state

of lagoons and eutrophication trends given the recent increase in the capacity of the sewage treatment plant.

AUTHOR CONTRIBUTIONS

M.L.: Methodology; Investigation; Visualization; Writing – review & editing;

D.L.: Resources; Investigation; Project Administration; Writing – review & editing;

A.N.: Investigation; Writing – review & editing;

L.A.: Data Curation; Writing – review & editing;

F.L.: Conceptualization; Supervision; Formal Analysis; Writing – original draft; Writing – review & editing.

REFERENCES

ABBOT, M. B. & BASCO, D. R. 1989. *Computational fluid dynamics, an introduction for engineers*. London: Longman Scientific & Technical.

ALVES, L. S., RAMOS V. V. A., LOBO, M. A. S., LAMEGO, F. & NAPOMUCENO, A. 2021. Reconstrução da história do processo da ocupação urbana e da eutrofização em lagoas do leste fluminense por registros sedimentaresitle [online]. *In:* COSTA, M. R., MONTEIRO-NETO, C., TUBINO, R. A. & ANGELINI, R. (eds.). *Pesca e sustentabilidade passado, presente e futuro*. Rio de Janeiro: AH Edições, pp. 27-40. Available at: https://gbm.uff.br/wp-content/uploads/sites/406/2022/03/Livro_SLLF_Pesca_Sustentabilidade.pdf. [Accessed: 2022 Jun 01].

ANDRIEUX-LOYER, F. & AMINOT, A. 2001. Phosphorus forms related to sediment grain size and geochemical characteristics in french coastal areas. *Estuarine, Coastal and Shelf Science*, 52(5), 617-629, DOI: https://doi.org/10.1006/ecss.2001.0766

ANDRIEUX-LOYER, F., PHILIPPON, X., BALLY, G., KÉROUEL, R., YOUENOU, A. & LE GRAND, J. 2008. Phosphorus dynamics and bioavailability in sediments of the Penzé Estuary (NW France): In relation to annual P-fluxes and occurrences of Alexandrium minutum. *Biogeochemistry*, 88(3), 213-231, DOI: https://doi.org/10.1007/s10533-008-9199-2

ANGELINI, R., NEPOMUCENO, A., COSTA, M. R., MONTEIRO-NETO, C., MORETTI, T., MONTEIRO, L. F. A., BELLO, M., SILVA, P. H. A., LEMA, M. C., ERBAS, T., ALVES, L., LAMEGO, F., ABRIL, G. & TUBINO, R. A. 2021. Integrando informações e dados em modelos ecológicos: buscando a padronização e o entendimento sistêmico [online]. *In:* COSTA, M. R., MONTEIRO-NETO, C., TUBINO, R. A. & ANGELINI, R. (eds.). *Pesca e sustentabilidade passado, presente e futuro*. Rio de Janeiro: AH Edições, pp. 131-146. Available at: https://gbm.uff.br/wp-content/uploads/sites/406/2022/03/Livro_SLLF_Pesca_Sustentabilidade.pdf. [Accessed: 2022 Jul 08].

ASPILA, K. I., AGEMIAN, H. & CHAU, A. S. Y. 1976. A semi-automated method for the determination of inorganic, organic and total phosphate in sediments. *Analyst*, 101(1200), 187-197.

AZEVEDO, M. N. S. 1987. *L'impact des politiques urbaines sur le développement de Niterói: 1960-1980*. MSc. Val de Marneu: Université Paris.

BARBIÉRE, E. B. 1981. O factor climatico nos sistemas territoriais de recreaçao.(Le facteur climatique et les bases régionales du tourisme). *Revista Brasileira de Geografia Rio de Janeiro*, 43(2), 145-265.

BORGES, A. V. 2005. Do we have enough pieces of the jigsaw to integrate CO_2 fluxes in the coastal ocean ? *Estuaries*, 28(1), 3-27.

BORGES, A. V. & ABRIL, G. 2012. Carbon dioxide and methane dynamics in estuaries. *Treatise on Estuarine and Coastal Science*, 5, 119-161, DOI: https://doi.org/10.1016/B978-0-12-374711-2.00504-0

BRAGA, F. F. 2003. Diagnóstico das alterações na bacia do Rio João Mendes, Niterói, RJ: gerados pelo crescimento urbano desordenado [online]. *In: X Simpósio Brasileiro de Geografia Física Aplicada*. São Gonçalo: UERJ-FFP. Available at: http://www.cibergeo.org/XSBGFA/eixo3/3.3/156/156.htm. [Accessed: YEAR Mo Day].

CASTELAO, R. M., CAMPOS, E. J. D. & MILLER, J. L. 2004. A modelling study of coastal upwelling driven by wind and meanders of the Brazil Current. *Journal of Coastal Research*, 20(3), 662-671, DOI: https://doi.org/10.2112/1551-5036(2004)20[662:amsocu]2.0.co;2

CERDA, M., NUNES-BARBOZA, C. D., SCALI-CARVALHO, C. N., ANDRADE-JANDRE, K. & MARQUES, A. N. 2013. Balance de nutrientes del sistema lagunar piratininga-itaipu (sudeste de Brasil): efectos del manejo del sistema através del intercambio con el agua de mar. *Latin American Journal of Aquatic Research*, 41(2), 226-238, DOI: https://doi.org/10.3856/vol41-issue2-fulltext-3

CERDA, M., SCALI, C., VALDÉS, J., MACARIO, K. D., ANJOS, R. M., VOGEL, V., LAMEGO, F. & NEPOMUCENO, A. 2016. Coupling fallout ^{210}Pb and stables isotopes ($\delta^{13}C$, $\delta^{15}N$) for catchment urbanization reconstruction in southeastern coastal zone of Brazil. *Journal of Radioanalytical and Nuclear Chemistry*, 310(3), 1021-1032, DOI: https://doi.org/10.1007/s10967-016-4876-4

CHAPRA, S. C. & DOLAN, D. M. 2012. Great Lakes total phosphorus revisited: 2. Mass balance modeling. *Journal of Great Lakes Research*, 38(4), 741-754, DOI: https://doi.org/10.1016/j.jglr.2012.10.002

CONLEY, D. J., PAERL, H. W., HOWARTH, R. W., BOESCH, D. F., SEITZINGER, S. P., HAVENS, K. E., LANCELOT, C. & LIKENS, G. E. 2009. Controlling eutrophication: phosphorus and nitrogen. *Science*, 323, 1014-1015.

COTOVICZ JUNIOR, L. C., BRANDINI, N., KNOPPERS, B. A., MIZERKOWSKI, B. D., STERZA, J. M., OVALLE, A. R. C. & MEDEIROS, P. R. P. 2013. Assessment of the trophic status of four coastal lagoons and one estuarine delta, eastern Brazil. *Environmental Monitoring and Assessment*, 185(4), 3297-3311, DOI: https://doi.org/10.1007/s10661-012-2791-x

COTOVICZ JUNIOR, L. C., MACHADO, E. D. C., BRANDINI, N., ZEM, R. C. & KNOPPERS, B. A. 2014. Distributions of total, inorganic and organic phosphorus in surface and recent sediments of the sub-tropical and semi-pristine Guaratuba Bay estuary, SE Brazil. *Environmental Earth Sciences*, 72(2), 373-386, DOI: https://doi.org/10.1007/s12665-013-2958-y

COTOVICZ, L. C., KNOPPERS, B. A., BRANDINI, N., SANTOS, S. J. C. & ABRIL, G. 2015. A strong CO_2 sink enhanced by eutrophication in a tropical coastal embayment (Guanabara Bay, Rio de Janeiro, Brazil). *Biogeosciences*, 12(20), 6125-6146, DOI: https://doi.org/10.5194/bg-12-6125-2015

COTOVICZ, L. C., VIDAL, L. O., REZENDE, C. E., BERNARDES, M. C., KNOPPERS, B. A., SOBRINHO, R. L., CARDOSO, R. P., MUNIZ, M., ANJOS, R. M., BIEHLER, A. & ABRIL, G. 2020. Carbon dioxide sources and sinks in the delta of the Paraíba do Sul River (Southeastern Brazil) modulated by carbonate thermodynamics, gas exchange and ecosystem metabolism during estuarine mixin. *Marine Chemistry*, 226, 103869, DOI: https://doi.org/10.1016/j.marchem.2020.103869

DHN (Departamento de Hidrografia e Navegação). 1987. *Cartas FB-1511-002/87 e FB-1511-003/87, Escala 1:10.000*. Rio de Janeiro: DHN.

DIAS, P. P. B. B., MARTINS, M. V. A., CLEMENTE, I. M. M. M., CARELLI, T. G., SILVA, F. S., FONTANA, L. F., LORIN, M. L., PANIGAI, G., PINHEIRO, R. H., MENDONÇA-FILHO, J. G. & LAUT, L. L. M. 2017. Assessment of the Trophic State of Saquarema Lagoonal System, Rio De Janeiro (Brazil). *Journal of Sedimentary Environments*, 2(1), 49-64, DOI: https://doi.org/10.12957/jse.2017.28194

DIAZ, R. J. & ROSENBERG, R. 2008. Spreading dead zones and consequences for marine ecosystems. *Science*, 321(5891), 926-929, DOI: https://doi.org/10.1126/science.1156401

DUPRA, V., SMITH, S. V., CROSSLAND, J. I. M. & CROSSLAND, J. C. 2000. Land-ocean interactions in the coastal zone (LOICZ). *Loicz Reports & Stuidies*, 15, 93, DOI: https://doi.org/10.13140/RG.2.1.2349.2322

ERBAS, T., MARQUES, A. & ABRIL, G. 2021. A CO_2 sink in a tropical coastal lagoon impacted by cultural eutrophication and upwelling. *Estuarine, Coastal and Shelf Science*, 263, 107633, DOI: https://doi.org/10.1016/j.ecss.2021.107633

FRANKIGNOULLE, M., ABRIL, G., BORGES, A., BOURGE, I., CANON, C., DELILLE, B., LIBERT, E. & THÉATE, J. M. 1998. Carbon dioxide emission from European estuaries. *Science*, 282(5388), 434-436, DOI: https://doi.org/10.1126/science.282.5388.434

GALLISSAIRES, J. M., ABUSSAMRA, E., TINOCO, T. & COE, R. 1990. Variações sazonais de perfis de Praia - Praias de Piratininga e Camboinhas (Niterói-RJ). *In: Anais do II Simpósio de Ecossistemas Da Costa Sul e Sudeste Brasileira: Estrutura, Função e Manejo*, Águas de Lindóia, São Paulo, 6-11 Apr 1990. Águas de Lindóia: ACIESP, pp. 352-356.

GALVÃO, R. S. 2008. *Drenagem urbana e planejamento ambiental: vale do rio João Mendes (Niterói/RJ)* [online]. MSc. Niterói: UFF-PPG (Universidade Federal Fluminense). Available at: https://app.uff.br/riuff/bitstream/handle/1/17277/Renata%20dos%20Santos-Dissert.pdf?sequence=1&isAllowed=y. [Accessed: 2022 Mar 27].

GAO, Y., CORNWELL, J. C., STOECKER, D. K. & OWENS, M. S. 2012. Effects of cyanobacterial-driven pH increases on sediment nutrient fluxes and coupled nitrification-denitrification in a shallow fresh water estuary. *Biogeosciences*, 9(7), 2697-2710, DOI: https://doi.org/10.5194/bg-9-2697-2012

HARRIS, G. P. 2001. Biogeochemistry of nitrogen and phosphorus in Australian catchments, rivers and estuaries. *Marine and Freshwater Research*, 52(1), 139-149.

HEINRICH, L., ROTHE, M., BRAUN, B. & HUPFER, M. 2021. Transformation of redox-sensitive to redox-stable iron-bound phosphorus in anoxic lake sediments under laboratory conditions. *Water Research*, 189, 116609, DOI: https://doi.org/10.1016/j.watres.2020.116609

JIAN, L., JUNYI, Y., JINGCHUN, L., CHONGLING, Y., HAOLIANG, L. & SPENCER, K. L. 2017. The effects of sulfur amendments on the geochemistry of sulfur, phosphorus and iron in the mangrove plant (Kandelia obovata (S. L.)) rhizosphere. *Marine Pollution Bulletin*, 114(2), 733-741, DOI: https://doi.org/10.1016/j.marpolbul.2016.10.070

KENNEY, W. F., WHITMORE, T. J., BUCK, D. G., BRENNER, M., CURTIS, J. H., DI, J. J., KENNEY, P. L. & SCHELSKE, C. L. 2014. Whole-basin, mass-balance approach for identifying critical phosphorus-loading thresholds in shallow lakes. *Journal of Paleolimnology*, 51(4), 515-528, DOI: https://doi.org/10.1007/s10933-014-9771-9

KIM, D. K., ZHANG, W., RAO, Y. R., WATSON, S., MUGALINGAM, S., LABENCKI, T., DITTRICH, M., MORLEY, A. & ARHONDITSIS, G. B. 2013. Improving the representation of internal nutrient recycling with phosphorus mass balance models: a case study in the Bay of Quinte, Ontario, Canada. *Ecological Modelling*, 256, 53-68, DOI: https://doi.org/10.1016/j.ecolmodel.2013.02.017

KJERFVE, B. & CESAR, A. R. 1997. Introduction. *Continental Shelf Research*, 17(13), 1609-1643.

KNOPPERS, B., KJERFVE, B. & CARMOUZE, J. P. 1991. Trophic state and water turn-over time in six choked coastal lagoons in Brazil. *Biogeochemistry*, 14(2), 149-166, DOI: https://doi.org/10.1007/BF00002903

KROON, F. J., KUHNERT, P. M., HENDERSON, B. L., WILKINSON, S. N., KINSEY-HENDERSON, A., ABBOTT, B., BRODIE, J. E. & TURNER, R. D. R. 2012. River loads of suspended solids, nitrogen, phosphorus and herbicides delivered to the Great Barrier Reef lagoon. *Marine Pollution Bulletin*, 65(4-9), 167-181, DOI: https://doi.org/10.1016/j.marpolbul.2011.10.018

KUCHLER, P., FERREIRA, A. P. S., SILVA, J. A. & SILVA, A. T. 2005. A análise da diminuição do espelho d'água das Lagoas de Itaipu e Piratininga com o subsídio do Sensoriamento Remoto. *In: Anais do 12º Simpósio Brasileiro de Sensoriamento Remoto (SBSR)*. Goiânia, Goiás, 16-21 Apr 2005. Goiás: INPE/UERJ-FFP, pp. 3651-3653.

MARKOVIC, S., LIANG, A., WATSON, S. B., GUO, J., MUGALINGAM, S., ARHONDITSIS, G., MORLEY, A. & DITTRICH, M. 2019. Biogeochemical mechanisms controlling phosphorus diagenesis and internal loading in a remediated hard water eutrophic embayment. *Chemical Geology*, 514, 122-137, DOI: https://doi.org/10.1016/j.chemgeo.2019.03.031

MARQUES JUNIOR, A., CRAPEZ, M. A. C., NUNES, C. D. & BARBOZA, A. 2006. Impact of the Icaraí Sewage Outfall in Guanabara Bay, Brazil. *Brazilian Archives of Biology and Technology*, 49(4), 643-650.

MEALS, D. W., CASSELL, E. A., HUGHELL, D., WOOD, L., JOKELA, W. E. & PARSONS, R. 2008. Dynamic spatially explicit mass-balance modeling for targeted watershed phosphorus management. II. Model application. *Agriculture, Ecosystems and Environment*, 127(3-4), 223-233, DOI: https://doi.org/10.1016/j.agee.2008.04.005

NITERÓI. 2019. *Relatórios de hidrologia: caracterização das vazões e dos aportes de cargas contribuintes ao sistema perilagunar piratininga-Itaipú/Niterói (Vols. 1–4)* [online]. Porto Alegre: Prefeitura de Niterói/HydroScience. Available at: http://www.prosustentavel.niteroi.rj.gov.br/pdf/RE_P2_HIDROLOGIA_1oSEM_V02.pdf. [Accessed: 2022 Feb 14].

NITERÓI. 2002. *Plano urbanístico da região oceânica* [online]. Rio de Janeiro: Prefeitura de Niterói. Available at: http://pgm.niteroi.rj.gov.br/legislacao_pmn/2002/LEIS/1968_Pur_da_Regiao_Oceanica.pdf. [Accessed: 2022 Mar 27].

NIXON, S. W. 1995. Coastal marine eutrophication: a definition, social causes, and future concerns. *Ophelia*, 41(1), 199-219, DOI: https://doi.org/10.1080/00785236.1995.10422044

OXMANN, J. F. & SCHWENDENMANN, L. 2015. Authigenic apatite and octacalcium phosphate formation due to adsorption-precipitation switching across estuarine salinity gradients. *Biogeosciences*, 12(3), 723-738, DOI: https://doi.org/10.5194/bg-12-723-2015

PAERL, H. W., HALL, N. S., PEIERLS, B. L. & ROS-SIGNOL, K. L. 2014. Evolving paradigms and challenges in estuarine and coastal eutrophication dynamics in a culturally and climatically stressed world. *Estuaries and Coasts*, 37(2), 243-258, DOI: https://doi.org/10.1007/s12237-014-9773-x

PÁEZ-OSUNA, F., PIÑÓN-GIMATE, A., OCHOA-IZA-GUIRRE, M. J., RUIZ-FERNÁNDEZ, A. C., RAMÍREZ--RESÉNDIZ, G. & ALONSO-RODRÍGUEZ, R. 2013. Dominance patterns in macroalgal and phytoplankton biomass under different nutrient loads in subtropical coastal lagoons of the SE Gulf of California. *Marine Pollution Bulletin*, 77(1-2), 274-281, DOI: https://doi.org/10.1016/j.marpolbul.2013.09.048

PAGLIOSA, P., FONSECA, A., BARBOSA, F. & BRAGA, E. 2006. Urbanization impact on subtropical estuaries: a comparative study of water properties in urban areas and in protected areas. *Journal of Coastal Research*, 2004(39), 731-735.

PANOSSO, R. 2001. The role of extracellular phosphatases in aquatic environments. *Oecologia Australis*, 9(1), 33-56.

PERES-NETO, P. R., JACKSON, D. A. & SOMERS, K. M. 2003. Giving meaningful interpretation to ordination axes: assessing loading significance in principal component analysis. *Ecology*, 84(9), 2347-2363, DOI: https://doi.org/10.1890/00-0634

PRATT, C., SHILTON, A., PRATT, S., HAVERKAMP, R. G. & EL-METRI, I. 2007. Effects of redox potential and pH changes on phosphorus retention by melter slag filters treating wastewater. *Environmental Science and Technology*, 41(18), 6585-6590, DOI: https://doi.org/10.1021/es070914m

RODRÍGUEZ-GALLEGO, L., ACHKAR, M., DEFEO, O., VIDAL, L., MEERHOFF, E. & CONDE, D. 2017. Effects of land use changes on eutrophication indicators in five coastal lagoons of the Southwestern Atlantic Ocean. *Estuarine, Coastal and Shelf Science*, 188, 116-126, DOI: https://doi.org/10.1016/j.ecss.2017.02.010

RSTUDIO TEAM. 2020. *RStudio: integrated development for R.* Boston: RStudio.

RUTTENBERG, K. C. 2003. The global phosphorus cycle. *Treatise on Geochemistry*, 8, 682.

SALVADOR, M. V. S. & SILVA, M. A. M. 2002. Morphology and sedimentology of the Itaipú embayment - Niterói/RJ. *Anais da Academia Brasileira de Ciencias*, 74(1), 127-134, DOI: https://doi.org/10.1590/S0001-37652002000100009

SAWYER, C. N., MCCARTY, P. L. & PARKIN, G. F. 2003. *Chemistry for environmental engineering and science*. 5th ed. London: McGraw-Hill Science/Engineering/Mat.

SOETAERT, K., HOFMANN, A. F., MIDDELBURG, J. J., MEYSMAN, F. J. R. & GREENWOOD, J. 2007. Reprint of "The effect of biogeochemical processes on pH". *Marine Chemistry*, 106(1-2spe), 380-401, DOI: https://doi.org/10.1016/j.marchem.2007.06.008

SOROKIN, Y. I. & SOROKIN, P. Y. 2010. Plankton of the central Great Barrier Reef: abundance, production and trophodynamic roles. *Journal of the Marine Biological Association of the United Kingdom*, 90(6), 1173-1187, DOI: https://doi.org/10.1017/S0025315410000597

SOUZA, M. F. L., KJERFVE, B., KNOPPERS, B., SOUZA, W. F. L. & DAMASCENO, R. N. 2003. Nutrient budgets and trophic state in a hypersaline coastal lagoon: Lagoa de Araruama, Brazil. *Estuarine, Coastal and Shelf Science*, 57(5-6), 843-858, DOI: https://doi.org/10.1016/S0272-7714(02)00415-8

STATHAM, P. J. 2012. Nutrients in estuaries - an overview and the potential impacts of climate change. *Science of the Total Environment*, 434, 213-227, DOI: https://doi.org/10.1016/j.scitotenv.2011.09.088

TIESSEN, H. 2008. Phosphorus in the global environment. *In:* WHITE, P. J. & HAMMOND, J. P. (eds.). *The ecophysiology of plant-phosphorus interactions*. New York: Springer, pp. 1-7.

UNEP/EARTH PRINT. 2009. Millennium ecosystem assessment. *In: An assessment of assessments: findings of the group of experts pursuant to UNGA Resolution 60/30* (Vol. 1). Nairóbi: UNEP/Earthprint.

YANG, S. & GRUBER, N. 2016. The anthropogenic perturbation of the marine nitrogen cycle by atmospheric deposition: nitrogen cycle feedbacks and the 15N Haber-Bosch effect. *Global Biogeochemical Cycles*, 30(10), 1418-1440, DOI: https://doi.org/10.1002/2016GB005421

ZHANG, W., KIM, D. K., RAO, Y. R., WATSON, S., MUGALINGAM, S., LABENCKI, T., DITTRICH, M., MORLEY, A. & ARHONDITSIS, G. B. 2013. Can simple phosphorus mass balance models guide management decisions? A case study in the Bay of Quinte, Ontario, Canada. *Ecological Modelling*, 257, 66-79, DOI: https://doi.org/10.1016/j.ecolmodel.2013.02.023